Galactic diffusion and wind models of cosmic-ray transport. I - Insight from CR composition studies and gamma-ray observations

Bloemen, J.B.G.M.; Dogiel, V.A.; Dorman, V.L.; Ptuskin, V.S.

Astron. Astrophys. 267, 372–387 (1993)

ASTRONOMY AND ASTROPHYSICS

Galactic diffusion and wind models of cosmic-ray transport

I. Insight from CR composition studies and γ-ray observations

J.B.G.M. Bloemen [1,2], V.A. Dogiel [3], V.L. Dorman [3], and V.S. Ptuskin [4]

[1] Space Research Leiden, P.O. Box 9504, 2300 RA Leiden, The Netherlands
[2] Leiden Observatory, P.O. Box 9513, 2300 RA Leiden, The Netherlands
[3] P.N. Lebedev Physical Institute of the Academy of Sciences, Leninsky Prospect 53, 117924 Moscow, Russia
[4] Institute of Terrestrial Magnetism, Ionosphere, and Radio Wave Propagation, 142092 Troitsk, Moscow Region, Russia

Received November 29, 1991; accepted March 9, 1992

Abstract. A two-dimensional model of the propagation of cosmic-ray (CR) nuclei in galaxies is discussed in which cosmic rays, produced in the galactic plane, diffuse into a halo and are convected outward in a galactic wind. Analytical solutions of the convection-diffusion equation are presented, assuming a linear increase of the convection velocity with distance from the plane, $V(z) = 3\,V_0\,z$, and allowing for an energy-dependent diffusion coefficient, $D(E) = D_0\,(E/\mathrm{GeV})^{\alpha}$. The differences compared to the classical diffusion model are outlined and constraints on model parameters from CR observations and γ-ray observations of the Milky Way are presented. A comparison of model predictions with the observed grammage traversed by cosmic rays and the abundance of radioactive ^{10}Be indicates that $V_0 \lesssim 15\,\mathrm{km\,s^{-1}\,kpc^{-1}}$ and $D_0 \approx (0.5\text{–}3) \times 10^{28}\,\mathrm{cm^2\,s^{-1}}$. An important consequence is that *the effective CR scale height in the solar vicinity has to be* $\lesssim 3$ kpc, independent of the presence of a Galactic wind. The lack of a strong Galacto-centric CR (proton) gradient, deduced from γ-ray analyses, indicates that these parameter values can only be representative for the Galaxy as a whole if the Galactic CR source distribution has a weak gradient as well. The radial distributions of potential CR sources such as supernova remnants and radio pulsars seem to show a too steep fall-off. We confirm that convection in a wind can lead to an increase of the halo size with kinetic energy of the nucleons, i.e., a hardening of the CR spectrum with distance from the plane (Lerche & Schlickeiser 1982). This may account for the observed hardening of the γ-ray spectrum with increasing latitude in the outer-Galaxy ($E_\gamma \gtrsim 300$ MeV) – assuming that the γ-ray emission is dominated by π^0-decay or electron bremsstrahlung – if the hardening of the CR spectrum starts sufficiently close to the plane (inside the gas disk). This requires $D_0 \lesssim 10^{27}\,\mathrm{cm^2\,s^{-1}}$ in order to limit the convection speed to reasonable values of $\lesssim 100\,\mathrm{km\,s^{-1}}$ within a few kpc from the Galactic plane.

Key words: cosmic rays – halos of galaxies – gamma rays – interstellar medium

1. Introduction

A variety of theoretical and observational studies has shown that the gaseous, magnetic-field, and cosmic-ray components of the interstellar medium in spiral galaxies can extend far beyond the disk into halo-type distributions. The physical relation between disk and halo, however, is still poorly unterstood. Not in the least this is the case for the cosmic-ray (CR) component. The two main scenarios to be distinguished (starting from the assumption that cosmic rays are produced in the disk) are that of a static halo, in which CR particles propagate by diffusion, and a dynamical halo, in which cosmic rays diffuse and are also convected outward in a galactic wind. Convective transport is provided by a directed flux of MHD waves to which the CR particles are coupled through intensive scattering (see review by Wentzel 1974). These waves may either be generated by the CR particles themselves or preexisting. One possible scenario is that of a large-scale flow of interstellar gas with a frozen-in magnetic field, but such an accompanying gas flow is not a prerequisite. Cosmic rays might help to drive a gas flow (Ipavich 1975; Axford 1981; Breitschwerdt et al. 1987), in addition to buoyancy and powering by supernovae (Mathews & Baker 1971; Chevalier & Oegerle 1979; McKee & Ostriker 1977; Heiles 1989). Formally, only gas flows faster than the galactic escape velocity, without cooling down and falling back to the galactic plane (Shapiro & Field 1976; Bregman 1980), can be referred to as galactic winds. In practice, the term wind models is used in CR astrophysics when the convection length scale is large compared to the thickness of the galactic gas disk, without the requirement that the gas actually escapes from the galaxy.

One most simple model, not yet mentioned above, is the leaky-box model, in which the distributions of all ingredients, such as the CR particles and their sources, the interstellar gas density, and the CR energy losses are assumed to be uniform throughout the confinement volume. The number density $N_i(E)$ of particles of type i, as a function of energy E, is in this model described by

$$\frac{N_i}{\tau} + \hat{B}_i(E)\,N_i = Q_i(E),$$

where τ is the leakage time of cosmic rays out of the Galaxy and $Q_i(E)$ the CR production rate. The operator $\hat{B}(E)$ describes energy losses in the interstellar medium, both of continuous as well as catastrophic (collisions) nature. This model is far from reality, but it has turned out to be of great value and is still of some use, as can be seen below.

A detailed development of the halo diffusion model was first presented by Ginzburg & Syrovatskii (1964), with further exten-

Send offprint requests to: J.B.G.M. Bloemen

sions and updates given by e.g. Cesarsky (1980) and Berezinsky et al. (1990). This halo diffusion model has turned out to be generally successful in accounting for most CR observations, both direct observations of particles near Earth as well as indirect observations via the diffuse radio-synchroton and γ-ray emission of our Galaxy and the radio emission of other galaxies. This does not imply that convection can be excluded. For instance, wind speeds of the order 10 km s^{-1} would provide a natural explanation of the form of the observed variation of the CR path length with energy (Jones 1979; Freedman et al. 1980; Kóta and Owens 1980). Also, possible indications of convective transport are found from recent spectral-index studies of radio and γ-ray surveys of our Galaxy (Reich & Reich 1988; Bloemen et al. 1988) and from radio studies of the edge-on galaxies NGC 4631 (Sukumar & Velusamy 1985; Werner 1988; Hummel & Dettmar 1990) and NGC 891 (Hummel et al. 1990), but further modelling is required.

First studies of CR transport in a dynamical model, mainly aimed at making a case for the very existence of a CR halo, were presented by Bulanov et al. (1972, Hillas (1975), and Jokipii (1976). Owens & Jokipii (1977) presented a Monte Carlo study of CR transport in a one-dimensional convection-diffusion model. Analytical studies of such a model were discussed by Jones (1979); Prishchep & Ptuskin (1979); Freedman et al. (1980), Kóta & Owens (1980) and Dogiel et al. (1980). The CR diffusion coefficient was taken to be uniform throughout the system. The wind speed was taken to be constant in the halo and zero in the source disk. Lerche & Schlickeiser (1982) considered a non-uniform velocity distribution for the wind, increasing with distance to the galactic plane, and a non-uniform diffusion coefficient. An important result of this work is the predicted spectral behaviour of the CR particles, and thus of the radio and γ-ray emission, in the halo and in the disk-halo interface, which contains signatures that can helpt to distinguish between a static halo and a dynamical halo.

Despite the vast amount of work on this topic, it is still unclear which model is to be preferred. The main aim of this paper is to present a complete set of analytical expressions for essentially all observable quantities in a two-dimensional convection-diffusion model. We concentrate here on particles that do not suffer radiative energy losses such as synchrotron and inverse-Compton losses (i.e., the proton-nuclear CR component and "low-energy" electrons), and consider the constraints set by observations of the grammage traversed by cosmic rays, radioactive nuclei, and the diffuse Galactic γ-ray emission. Preliminary results have been presented by Bloemen et al. (1991 a, b). Paper II will be focussed on (high-energy) electrons. In order to illustrate the impacts of a wind in comparison with a pure diffusion model, we also discuss throughout our findings in the limit of diffusion-dominated propagation. Section 2 describes the main characteristics of the model we consider and presents our results for protons (and low-energy electrons). Section 3 addresses nuclei subject to fragmentation and Sect. 4 deals with radioactive secondary nuclei. In Sect. 5 the observational constraints from the previous two sections are combined and in Sect. 6 constraints from γ-ray observations of the Milky Way are discussed.

2. Protons and low-energy electrons

2.1. The general solution

For CR particles that are not subject to radioactive decay and catastrophic energy losses (collisions with interstellar gas nuclei), the density distribution $N(E, \boldsymbol{r})$ is given by a continuity equation of the form

$$-\nabla(\hat{D}(E,\boldsymbol{r})\,\nabla N - V(\boldsymbol{r})N) - \frac{\partial}{\partial E}\left(\frac{\mathrm{div}\,V}{3}EN\right) - \frac{\partial}{\partial E}(\dot{E}(E,\boldsymbol{r})N) = Q(E,\boldsymbol{r}), \quad (1)$$

where E is the kinetic energy and $\boldsymbol{r}$ is the position in the galaxy. The first term of this equation describes spatial diffusion, characterized by the diffusion tensor $\hat{D}(E,\boldsymbol{r})$. We assume throughout that diffusion is isotropic and independent of position in the galaxy, so

$$\hat{D} = \begin{pmatrix} D_{RR} & D_{Rz} \\ D_{zR} & D_{zz} \end{pmatrix} = \begin{pmatrix} D_0 E^\alpha & 0 \\ 0 & D_0 E^\alpha \end{pmatrix}, \quad (2)$$

where D_0 is the normalization factor at $E = 1$ GeV. The second term describes convective transport with a convection speed $V(\boldsymbol{r})$, which we assume, for simplicity, to increase linearly with distance z from the midplane

$$V(z) = 3\,V_0\,z\,. \quad (3)$$

The third term describes adiabatic losses and the fourth term continuous energy losses (such as synchrotron and inverse-Compton losses, with $\dot{E} = -bE^2$). We limit our study in this paper to particles that are not subject to these losses (i.e., the proton-nuclear CR component and low-energy electrons), so we can adopt $\dot{E} = 0$. The right-hand side of Eq. (1) contains the source term. We assume that the particles originate at $z = 0$ (no re-acceleration outside) with a power-law spectrum, so

$$Q(E,R,z) = 2z_s K E^{-\gamma_0}\delta(z)\,f(R)\,, \quad (4)$$

where $2z_s$ is the thickness of the source disk, $f(R)$ describes the distribution of CR sources as a function of galacto-centric radius, and K and γ_0 characterize the differential number density of the particles. As boundary conditions we set the CR density equal to zero at the halo edges,

$$N(E, R = R_h, z) = 0$$
$$N(E, R, |z| = z_h) = 0\,, \quad (5)$$

where R_h is the radius of the halo volume and z_h its z-extent. This implies free escape of the particles into intergalactic space, where the CR number density is adopted to be negligibly small. Although these boundary conditions are rather arbitrary (z_h and R_h might be functions of energy, depending upon the conditions in intergalactic space; see Dogiel et al. 1991), we see below that they do not have a major impact on our results. The general solution of the two-dimensional convection-diffusion equation is given in Appendix A.

2.2. The one-dimensional solution

Here we discuss the illustrative, one-dimensional version of the convection-diffusion model, for which the continuity Eq. (1) reduces to

$$-\frac{\partial}{\partial z}\left(D(E)\frac{\partial}{\partial z}N - VN\right) - \frac{\partial}{\partial E}\left(\frac{1}{3}\frac{\mathrm{d}V}{\mathrm{d}z}EN\right) = Q(E,z)\,, \quad (6)$$

with

$$D(E) = D_0 E^\alpha, \quad (7)$$
$$V(z) = 3\,V_0\,z\,, \quad (8)$$
$$Q(E,z) = 2z_s K E^{-\gamma_0}\delta(z) \quad (9)$$

[similar to the model studied by Lerche & Schlickeiser (1982), although they allowed more freedom in the z-dependence of V and D]. The boundary conditions are

$$N(E, |z| = z_h) = 0 \tag{10}$$

$$-2\frac{\partial}{\partial z}(D(E)N)\Big|_{z=0} = 2 z_s K E^{-\gamma_0}. \tag{11}$$

With these boundary conditions, the solution of Eq. (6) is

$$N(E,z) = \frac{z_s K E^{-(\gamma_0+\alpha)}}{D_0} \cdot \left(z_h \frac{{}_1F_1\left(\frac{p+1}{2}, \frac{3}{2}, \xi_h^2\right)}{{}_1F_1\left(\frac{p}{2}, \frac{1}{2}, \xi_h^2\right)} {}_1F_1\left(\frac{p}{2}, \frac{1}{2}, \xi^2\right) - z\, {}_1F_1\left(\frac{p+1}{2}, \frac{3}{2}, \xi^2\right)\right), \tag{12}$$

where ${}_1F_1(a,b,x)$ is a confluent hypergeometrical function [1] and

$$p = \frac{\gamma_0 + 2 + \alpha/2}{3 + \alpha/2}, \tag{13}$$

$$\xi^2 = \frac{z^2 (3+\alpha/2) V_0}{2 D_0 E^\alpha}, \tag{14}$$

$$\xi_h^2 = \frac{z_h^2 (3+\alpha/2) V_0}{2 D_0 E^\alpha}. \tag{15}$$

This solution is characterized by two dimensionless parameters

$$\xi^2 = \frac{z}{z_c^2(E)} \quad \text{and} \quad \xi_h^2 = \frac{z_h^2}{z_c^2(E)}, \tag{16}$$

with

$$z_c(E) = \sqrt{\frac{2 D_0 E^\alpha}{(3+\alpha/2) V_0}}, \tag{17}$$

which is essentially the boundary between a diffusion dominated regime ($z < z_c$) and a convection dominated regime ($z > z_c$). This can easily be seen if one realizes that diffusion takes a particle a distance z away from the disk in a time z^2/D. This is equal to the time scale for adiabatic cooling [2], $1/V_0$, for a distance $z_c = (D/V_0)^{1/2}$, which is similar to z_c as defined above [an accurate evaluation of (6) gives the additional factor]. The convection time scale is of the same order as the time scale for adiabatic cooling, namely $1/(3V_0)$. Hence, diffusion is the fastest way to travel for $z < z_c$ and convection is faster for $z > z_c$, which we may call, therefore, diffusion and convection dominated regimes.

The following approximations to the solution (12) can be made, using the expressions of ${}_1F_1$ given in footnote (1).

(a) If $z \ll z_c(E)$ and $z_h \ll z_c(E)$ ($\xi \ll 1$ and $\xi_h \ll 1$), then

$$N(E,z) \simeq \frac{z_s K}{D_0} E^{-(\gamma_0+\alpha)} (z_h - z). \tag{18a}$$

The distribution approaches the solution of the pure diffusion model. Convection is unimportant.

(b) If $z \ll z_c(E)$ and $z_h \gg z_c(E)$ ($\xi \ll 1$ and $\xi_h \gg 1$), then

$$N(E,z) \simeq \frac{z_s K}{D_0} E^{-(\gamma_0+\alpha)} (A z_c(E) - z) \propto E^{-(\gamma_0+\alpha/2)},$$

$$\text{with} \quad A = \frac{\Gamma\left(\frac{3}{2}\right)\Gamma\left(\frac{p}{2}\right)}{\Gamma\left(\frac{1}{2}\right)\Gamma\left(\frac{p+1}{2}\right)}, \tag{18b}$$

where A is close to unity. The impact of convection becomes visible because the boundary of the effective diffusion halo z_c is well inside the halo boundaries ($z_c \ll z_h$), but z is inside the diffusion dominated regime ($z \ll z_c$).

(c) If $z \gg z_c(E)$ and $z_h \gg z_c(E)$ ($\xi \gg 1$ and $\xi_h \gg 1$), then

$$N(E,z) \propto E^{-(6\gamma_0+\alpha)/(6+\alpha)}\, z^{-(2\gamma_0+\alpha+4)/(6+\alpha)}. \tag{18c}$$

z is outside the boundary of the effective diffusion halo and in the convection dominated regime. The CR density decreases rapidly, which implies that the boundary conditions at $z = z_h$ are relatively unimportant.

The same behaviour of the CR spectrum (18b, c) was found by Lerche & Schlickeiser (1982) for the boundaryless case (see end of Appendix A). A comparison of (18a) with (18b) and (18c) shows an essential difference between the spectral behaviour of static and dynamical models: whereas in the diffusion model the spectral shape is uniform (at least for the low-energy electrons and the proton-nuclear CR component we are considering here), in the convection-diffusion model the spectral index changes as a function of distance from the galactic plane. A closer look at (18) shows that the spectrum flattens with increasing z. For example, with typical (local Galactic) estimates of $\gamma_0 \simeq 2.1 - 2.3$ and $\alpha \simeq 0.6$, this amounts to a change in the spectral index γ of ~ 0.4 between $z \ll z_c$ and $z \gg z_c$. The basic physical reason for this spectral behaviour is the increase of the size of the effective diffusion halo with increasing energy, $z_c \propto E^{\alpha/2}$ (17), resulting from the fact that the diffusion coefficient increases with energy. If $D(E) = D_0$ (i.e., $\alpha = 0$), z_c is independent of energy and the spectral shape does not change with z. In fact, since the propagation time to the boundary of the effective diffusion halo is now independent of energy, the spectral index is equal to that of the source spectrum, $\gamma = \gamma_0$, independent of z, as is evident from (18b, c).

Figures 1 and 2 show some examples of solutions of (6). Note that with increasing energy as well as decreasing convection speed (i.e., in both cases, large z_c), $N(E,z)$ is less influenced by convection and approaches the expected distribution for pure diffusion, given by equation (18a), as argued above.

High-energy electrons will be discussed in Paper II, but it may be illustrative at this point to describe briefly the wellknown behaviour of the halo size of high-energy electrons in the pure diffusion model (e.g., Ginzburg & Syrovatskii 1964), which shows close resemblance to the above. The competitive time scales in this case are the diffusion travel time to a certain point z above the disk, z^2/D, and the time for synchrotron and inverse-Compton losses, $(bE)^{-1}$ (Sect. 2.1). These are equal at a distance $z_d = [D/(bE)]^{1/2} \propto E^{(\alpha-1)/2}$. Again, this distance can be interpreted as the boundary of an effective diffusion halo, but now decreasing with energy (if $\alpha < 1$, as supported by observations).

It can be seen from the above that $N(E,z)$ is determined by three main parameters: D_0, V_0, and z_h. In the following sections we try to set observational constraints on these parameters.

---

[1] We frequently use the approximation ${}_1F_1(a,b,x) \simeq \frac{\Gamma(b)}{\Gamma(a)} e^x x^{a-b}$ for $x \gg 1$ and ${}_1F_1(a,b,x) \simeq 1$ for $x \ll 1$ (see, e.g., Abramowitz & Stegun 1972).

[2] The energy-loss rate due to adiabatic deceleration can be written as $\dot{E} = -\frac{1}{3}\frac{dV}{dz}E = -V_0 E$.

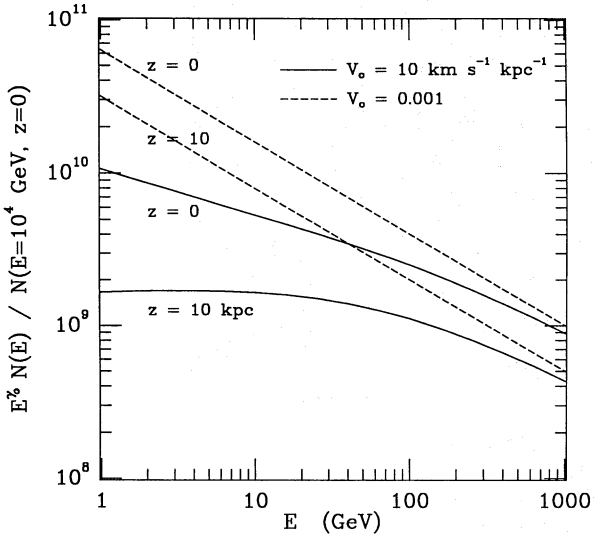

Fig. 1. Examples of energy spectra (multiplied by E^{γ_0}) in a 1-D convection-diffusion model for CR particles that do not suffer radiative losses. Spectra are shown at $z = 0$ and 10 kpc for models with $V_0 = 10$ and 0.001 km s^{-1} kpc^{-1} (the latter approaches the pure diffusion model). Other parameter values are: $D_0 = 10^{29}$ cm^2 s^{-1}, $z_h = 20$ kpc, $\gamma_0 = 2.1$, and $\alpha = 0.6$. The parameter values were chosen such that the asymptotic behaviour sketched in Sect. 2.2 is clearly visible

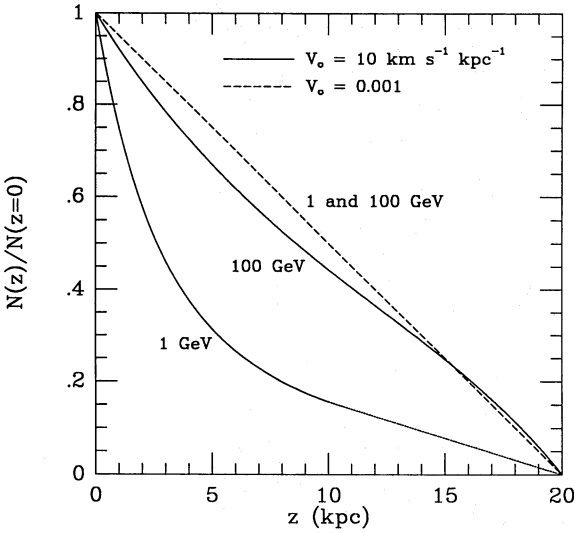

Fig. 2. Examples of z-distributions in a 1-D convection-diffusion model for CR particles that do not suffer radiative losses. Distributions are shown at $E = 1$ and 100 GeV for models with $V_0 = 10$ and 0.001 km s^{-1} kpc^{-1} (the latter approaches the pure diffusion model). Other parameter values are same as in Fig. 1

3. Nuclei subject to fragmentation: constraints from grammage

An important observational constraint on CR propagation is the grammage X, i.e., the mean matter thickness traversed by cosmic rays before reaching the Earth. This quantity can be derived from the ratio of the intensity of primary CR nuclei (ejected by the CR sources), to that of secondary CR nuclei, which are generated through collisions of the primaries with interstellar gas nuclei. Observations show that $X \approx 6-8$ g cm^{-2} for particles with energies $\lesssim 1$ GeV/nuc and that X decreases with energy above ~ 1 GeV/nuc, following approximately an $E^{-0.5}$ relationship (see, e.g., Garcia-Munoz et al. 1987; Webber et al. 1990). In case of CR reacceleration in the ISM (not considered here), the value of X may be somewhat smaller and the dependence on energy may be weaker (e.g. Cesarsky 1987).

We can determine X in the framework of the convection-diffusion model by including in Eq. (6) a term $2z_g n_g v\sigma\delta(z)N$ describing the interaction of the primaries with gas in the disk,

$$-\frac{\partial}{\partial z}\left(D(E)\frac{\partial}{\partial z}N - VN\right) - \frac{\partial}{\partial E}\left(\frac{1}{3}\frac{dV}{dz}EN\right) + 2z_g n_g v\sigma\delta(z)N = Q(E,z), \quad (23)$$

with $D(E)$, $V(z)$, and $Q(E,z)$ given by (7), (8), and (9). In the fragmentation term, z_g and n_g are the half thickness and average number density of the gas disk, σ is the cross section of the fragmentation process, and v is the particle velocity. The solution of (23) is given in Appendix B (Eq. B8). For $z = 0$ (the point of interest here), it reduces to

$$N(E,0) = \frac{z_s z_h K E^{-(\gamma_0+\alpha)}}{D_0}\sum_{n=0}^{\infty}(-1)^n\left(\frac{z_g z_h n_g v\sigma}{D_0 E^\alpha}\right)^n \cdot \prod_{k=0}^{n}\frac{{}_1F_1\left(\frac{p_k+1}{2},\frac{3}{2},\xi_h^2\right)}{{}_1F_1\left(\frac{p_k}{2},\frac{1}{2},\xi_h^2\right)}, \quad (24)$$

with

$$p_k = \frac{\gamma_0 + 2 + \frac{k+1}{2}\alpha}{3+\frac{\alpha}{2}} \quad (25)$$

and $\xi_h^2 = z_h^2/z_c^2$ (Sect. 2.2).

In the limit of the pure diffusion model ($\xi_h \ll 1$), Eq. (24) is equivalent to (see footnote 1)

$$N(E,0) = \frac{z_s z_h K E^{-(\gamma_0+\alpha)}}{D_0}\sum_{n=0}^{\infty}(-1)^n\left(\frac{z_g z_h n_g v\sigma}{D_0 E^\alpha}\right)^n, \quad (26)$$

which shows close resemblance to the solution of the classical leaky-box model, frequently used for CR composition studies. This becomes clear if one realizes that the solution of the leaky-box equation

$$N = \frac{q\tau}{1+\sigma X} \quad (27)$$

can be written as

$$N = q\tau\sum_{n=0}^{\infty}(-1)^n(\sigma X)^n, \quad (28)$$

where q is the CR production rate, τ the leakage time out of the galaxy, and X the "grammage", defined as $X = n v \tau$. *Here (and in the following) X is in units of cm^{-2}.* A comparison of (26) and (28) shows that we can define X in the diffusion limit of the convection-diffusion model as

$$X = \frac{z_g z_h n_g v}{D_0 E^\alpha}, \quad (29)$$

which is the wellknown expression of X in the pure diffusion model for $\sigma X < z_h/z_g$ (e.g. Berezinsky et al. 1990). Formally,

convergence of (28) requires $\sigma X < 1$. If $N(\sigma)$ is an analytical function, however, the expression

$$N(E,0) = \frac{z_s z_h K E^{-(\gamma_0+\alpha)}}{D_0} \cdot \frac{1}{1+\sigma X}$$

is valid for any value of $\sigma X \neq -1$.

If convection plays a role ($\xi_h \gg 1$) then (24) can be approximated by

$$N(E,0) = \frac{z_s z_h K E^{-(\gamma_0+\alpha)}}{D_0} \sum_{n=0}^{\infty} (-1)^n \left(\frac{z_g z_c n_g v\sigma}{D_0 E^\alpha}\right)^n \cdot \prod_{k=0}^{n} \frac{\Gamma(\frac{3}{2})\,\Gamma(p_k/2)}{\Gamma(\frac{1}{2})\,\Gamma((p_k+1)/2)}. \quad (30)$$

Note that in the sum z_c appears instead of z_h (26). In this case the model is not reduced to the leaky box [because of the product factor, the expansion in Eq. (30) is not equivalent to that in (28)]. Using only the first terms of the summation, however, in which case (30) shows again close resemblance to the leaky-box equation (27, 28), one finds

$$X = \frac{z_g z_c n_g v}{D_0 E^\alpha} \frac{\Gamma(\frac{3}{2})\,\Gamma(p_1/2)}{\Gamma(\frac{1}{2})\,\Gamma((p_1+1)/2)}. \quad (31)$$

It can be verified that this is a reasonable approach by comparing this expression for X with the mean matter thickness $\langle X\rangle$ traversed by cosmic rays, defined as

$$\langle X\rangle = \left(-\frac{1}{N}\frac{\partial N}{\partial \sigma}\right)\Big|_{\sigma=0} \quad (32)$$

(Berezinsky et al. 1990), where $N(\sigma)$ stands for the moment generating function in probability theory. In the leaky-box model (N given by (27)) $\langle X\rangle = X$. Also in the convection-diffusion model (N given by (24)), it follows that $\langle X\rangle = X$, with X given by (29) and (31).

In summary, the above illustrates that

(a) if $\xi_h \ll 1$ (diffusion dominates) $X \propto \frac{z_h}{D_0 E^\alpha}$, and

(b) if $\xi_h \gg 1$ (convection is important)

$$X \propto \frac{z_c(E)}{D_0 E^\alpha} \propto (V_0 D_0 E^\alpha)^{-1/2}.$$

Note that the halo boundary z_h in the diffusion-dominated case is in fact replaced by the extent z_c of the effective diffusion halo in case convection is important. Also, note the weaker dependence on E if convection is important. Because of the decreasing impact of convection with energy (Sect. 2.2), this may offer a natural explanation of the form of the observed variation of X with energy, already pointed out by Jones (1979).

We see from the above that measurements of X set constraints on V_0 and D_0. Figure 3 shows the relation between V_0 and D_0 that is required in the convection-diffusion model in order to obtain a grammage of 6–8 g cm^{-2} at $E \lesssim 1$ GeV/nuc. We have used here the general solution (24) for $D = D_0$ (i.e., $\alpha = 0$):

$$N(E,0) = \frac{z_s z_h K E^{-\gamma_0}}{D_0} \sum_{n=0}^{\infty} (-1)^n \cdot \left(\frac{z_g z_h n_g v\sigma}{D_0} \frac{{}_1F_1((p+1)/2, \frac{3}{2}, \xi_h^2)}{{}_1F_1(p/2, \frac{1}{2}, \xi_h^2)}\right)^n, \quad (33)$$

with

$$p = \frac{\gamma_0 + 2}{3} \quad (34)$$

$$\xi_h^2 = \frac{3 z_h^2 V_0}{2 D_0} \quad (35)$$

$$z_c = \sqrt{\frac{2D_0}{3V_0}}, \quad (36)$$

giving

$$X = \frac{z_g z_h n_g v}{D_0} \frac{{}_1F_1((p+1)/2, \frac{3}{2}, \xi_h^2)}{{}_1F_1(p/2, \frac{1}{2}, \xi_h^2)}. \quad (37)$$

The asymptotic behaviour sketched above is clear from Fig. 3. We used $z_g n_g = 4\ 10^{20}$ cm^{-2}. Further discussion is given in Sect. 5.

The similarity of our diffusion-convection model and the leaky-box model, which is basically due to the delta approximations of the spatial distributions of the gas and the CR sources (see Berezinsky et al. 1990; Ptuskin & Soutoul 1990), is of particular interest because it implies that one can use the empirical leaky-box model to deduce X from observations and still interpret the obtained value in terms of the convection-diffusion model.

4. Constraints from radioactive nuclei

Another important constraint on CR propagation models is set by long-lived radioactive isotopes of the secondary CR component, for which in particular ^{10}Be (life time at rest $\tau \approx 2.2\ 10^6$ yr) is suitable (see, e.g., review by Simpson & Garcia-Munoz 1988). We investigate here which parameters of the convection-diffusion model are constrained by measurements of abundances of radioactive nuclei.

Again, we consider the one-dimensional model and restrict ourselves to nuclei with kinetic energies $E \lesssim 1$ GeV/nuc ($D = D_0$), to which most of the abundance measurements of radioactive nuclei are limited (the general solution of the two-dimensional transport equation, with energy dependent diffusion coefficient, is given in Appendix C). The equation describing the density distribution of radioactive CR nuclei, $N(E,z)$, produced through CR interactions with interstellar gas, can then be written as

$$-D_0 \frac{\partial^2}{\partial z^2} N + 3V_0 \frac{\partial}{\partial z}(zN) - V_0 \frac{\partial}{\partial E}(EN) + \frac{N}{\tau} = Q(E,z), \quad (38)$$

where we neglect the nuclear fragmentation of decaying nuclei. Q is the production rate of (radioactive) secondary nuclei by primary nuclei. Since the spatial distribution of the primary particles only weakly depends on the fragmentation cross sections, we approximate Q by

$$Q(E,z) = 2 z_g n_g v\sigma N_p(E,z)\,\delta(z), \quad (39)$$

where $N_p(E,z)$ is the distribution of protons, given by (12), with $\alpha = 0$, and σ is the effective production cross section. In the limit $\tau \to \infty$, (38) describes the density distribution of stable (non-radioactive) secondaries, $N_{\tau\to\infty}(E,z)$. The solution of (38) is similar to (12) (with $D = D_0$ and $\alpha = 0$). At $z = 0$ (the point of interest here), we find for stable secondary particles

$$N_{\tau\to\infty}(E,0) = \frac{z_h z_g n_g v\sigma N_p(E,0)}{D_0} \cdot \frac{{}_1F_1((p+1)/2, \frac{3}{2}, \xi_h^2)}{{}_1F_1(p/2, \frac{1}{2}, \xi_h^2)}, \quad (40)$$

with

$$p = \frac{\gamma_0 + 2}{3} \quad \text{and} \quad \xi_h^2 = \frac{3 z_h^2 V_0}{2 D_0}$$

and for the radioactive component

$$N_\tau(E,0) = \frac{z_h z_g n_g v \sigma N_p(E,0)}{D_0} \frac{{}_1F_1\,((p^*+1)/2, \frac{3}{2}, \xi_h^2)}{{}_1F_1\,(p^*/2, \frac{1}{2}, \xi_h^2)}, \tag{41}$$

with

$$p^* = \frac{\gamma_0 + 2 + 1/(V_0 \tau)}{3}.$$

Hence, near Earth and for $E \lesssim 1$ GeV/nuc, the fraction of non-decayed radioactive nuclei of a certain isotope is given by

$$f \equiv \frac{N_\tau}{N_{\tau\to\infty}} = \frac{{}_1F_1\,((p^*+1)/2, \frac{3}{2}, \xi_h^2)}{{}_1F_1\,(p^*/2, \frac{1}{2}, \xi_h^2)} \frac{{}_1F_1\,(p/2, \frac{1}{2}, \xi_h^2)}{{}_1F_1\,(p+1/2, \frac{3}{2}, \xi_h^2)}, \tag{42}$$

where $N_{\tau\to\infty}$ is the density of the nuclei under the assumption that the particles are stable. In the limit $\xi_h \ll 1$ (diffusion dominates), this fraction is equal to

$$f \approx \frac{\sqrt{D_0 \tau}}{z_h}, \tag{43}$$

as in the pure diffusion model (e.g. Ginzburg and Ptuskin 1976). If convection is important ($\xi_h \gg 1$) (42) reduces to

$$f \approx \frac{\Gamma(p^*/2)\,\Gamma((p+1)/2)}{\Gamma((p^*+1)/2)\,\Gamma(p/2)} \approx \sqrt{3 V_0 \tau}. \tag{44}$$

Note that (44) is approximately equivalent to (43), with z_h replaced by z_c. We see from the above that measurements of abundance ratios like ^{10}Be/^{9}Be set constraints on V_0 or D_0. The observed ratio ^{10}Be/^{9}Be gives $f \approx 0.25 \pm 0.1$ for rigidities of ~ 1 GV (see, e.g., Simpson & Garcia-Munoz 1988). Using (44) we find that this requires $V_0 \approx 10\,\mathrm{km\,s^{-1}\,kpc^{-1}}$ if $\xi_h \gg 1$. The exact evaluation [using (42)] is included in Fig. 3.

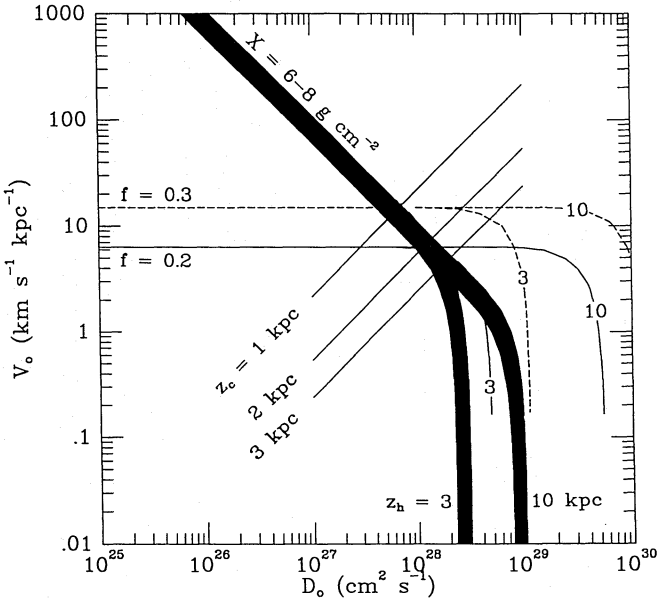

Fig. 3. Constraints on the relation between V_0 and D_0 in a convection-diffusion model from the observed CR grammage X and the observed abundance of Be isotopes (f is the surviving fraction of the radioactive isotope ^{10}Be). Note that the extent of the halo z_h only plays a role in the diffusion-dominated regime (the lower-right quadrant of the figure). See discussion in Sect. 5

5. Combined constraints from grammage and radioactive nuclei

Figure 3 enables a direct comparison of the constraints on V_0 and D_0 obtained from the observed grammage of cosmic rays with energies $\lesssim 1$ GeV/nuc (Sect. 3) and the abundance of the ^{10}Be isotope (Sect. 4). It can be concluded from this figure that in order to explain both the observed grammage and the abundance of ^{10}Be, it is necessary that $V_0 \lesssim 15\,\mathrm{km\,s^{-1}\,kpc^{-1}}$ and $D_0 \approx (0.5\text{–}3) \times 10^{28}\,\mathrm{cm^2\,s^{-1}}$. These estimates are consistent with the findings of Prischep & Ptuskin (1979) and Freedman et al. (1980). They assumed a constant convection velocity and found $V \approx 15\text{–}20\,\mathrm{km\,s^{-1}}$.

A very interesting implication for the effective z-extent of the CR halo in the solar vicinity can be seen from Fig. 3 as well. For this purpose we have included lines of constant z_c (reminder: beyond z_c the CR density drops rapidly). We see: (1) for $V_0 \approx 10\,\mathrm{km\,s^{-1}\,kpc^{-1}}$, the parameter z_h is not constrained, but $z_c \lesssim 3$ kpc and (2) for $V_0 < 10\,\mathrm{km\,s^{-1}\,kpc^{-1}}$, the parameter z_c is not constrained, but $z_h \lesssim 3$ kpc. In the latter, diffusion dominated case, the constraint on z_h can be directly seen by combining Eq. (29) and (43), which gives

$$z_h \approx \frac{z_g n_g v \tau}{X f^2},$$

i.e., $z_h \approx 1\text{–}3$ kpc for $X \approx 6\text{–}8\,\mathrm{g\,cm^{-2}}$ and $f \approx 0.25 \pm 0.1$ (using $z_g n_g \approx 4\ 10^{20}\,\mathrm{cm^{-2}}$). It can be concluded that *the effective scale height of the CR halo at ~ 1 GeV is $\lesssim 3$ kpc*. If we have underestimated $z_g n_g$ (the value we used here corresponds to the well known average column density of the disk gas towards the Galactic poles), the halo extent z_h can be larger than 3 kpc in the extreme case (i.e., both X and f small). Even then, however, it is unlikely that the effective CR scale height exceeds 3 kpc.

6. Constraints from γ-ray observations

6.1. The radial CR gradient

A further constraint on models of CR origin and propagation is set by the weak Galacto-centric gradient of the CR distribution, derived from correlation analyses of the COS-B γ-ray data and H I and CO gas tracer data (Bloemen et al. 1986; Strong et al. 1988). In the Galactic disk, the diffuse γ-ray emission at energies $\gtrsim 50$ MeV originates predominantly from CR-matter interactions via the bremsstrahlung and π°-decay processes (see, e.g., review by Bloemen 1989). The π°-decay process, initiated by the interaction of CR nuclei (mainly 1–10 GeV protons) with interstellar matter, probably dominates at the high energies ($E_\gamma \gtrsim 100$ MeV) we consider here. Dogiel & Uryson (1988) have compared the weak radial CR gradient with the predictions from a pure diffusion model. Assuming a CR source distribution resembling that of supernova-remnants (SNR's; Kodaira 1974), which has a much stronger radial gradient than the CR distribution derived from the COS-B data, it was found [see extension of this work by Dogiel and Bloemen reported in the review by Bloemen (1989)] that the lack of a strong CR gradient can only be explained (although marginally) if an extensive CR halo exists

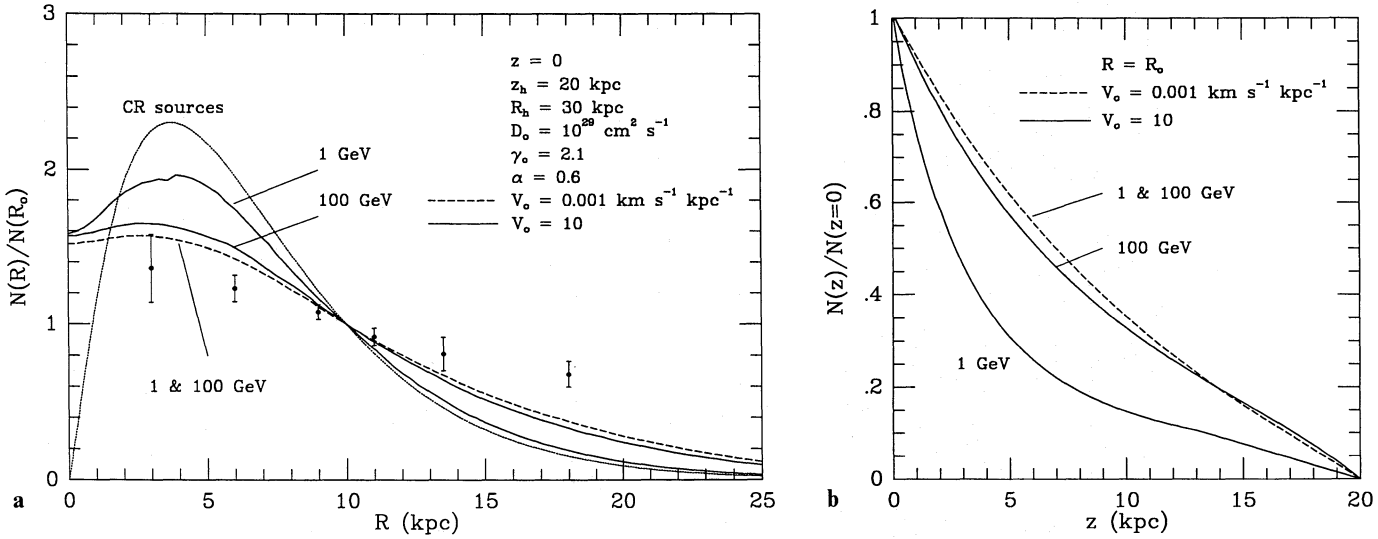

Fig. 4a and b. Examples of Galactocentric distributions **a** and z-distributions **b** of the CR density for $E = 1$ and 100 GeV in two-dimensional convection-diffusion models with $V_0 = 10$ and 0.001 km s^{-1} kpc^{-1} (the latter approaches the pure diffusion model). A SNR-like CR source distribution was chosen (dotted curve). The data points indicate the γ-ray emissivities derived by Strong et al. (1988) from a correlation analysis of the COS-B γ-ray survey and H I and CO surveys. All quantities are normalized at the radius of the solar circle (10 kpc)

($R_h \gtrsim 30$ kpc, $z_h \gtrsim 20$ kpc). In case of a small halo, the CR distribution is similar to the source distribution, because the probability to escape from the Galaxy is large and the CR density at a certain location is mainly determined by the local source density and the characteristics of the ambient interstellar medium. Stecker & Jones (1977) have performed a similar analysis of the SAS-2 data and derived an upper limit to the CR scale height at GeV energies of only ~ 3 kpc. The reason for this differing results is that the radial CR distribution derived from the SAS-2 data at that time showed a significantly stronger fall-off with Galactic radius than the one derived from the recent COS-B analyses mentioned above (for further details on this issue, see discussion by Bloemen, 1989).

Here we consider the impact of including convective effects, using the two-dimensional solution of the convection-diffusion model for protons, presented in Appendix A. This solution is complex, but can be approximated (for small α; see end of Appendix A), by

$$N(E,R,z) = \frac{2 z_s K E^{-(\gamma_0+\alpha)}}{D_0} \sum_j J_0(\nu_j R/R_h) \frac{\int_0^1 x J_0(\nu_j x) f(x R_h)\,dx}{J_1^2(\nu_j)} \left(z_h \frac{{}_1F_1((p+1)/2, \frac{3}{2}, \xi_h^2)}{{}_1F_1(p/2, \frac{1}{2}, \xi_h^2)} {}_1F_1\left(\frac{p}{2}, \frac{1}{2}, \xi^2\right) - z\, {}_1F_1\left(\frac{p+1}{2}, \frac{3}{2}, \xi^2\right)\right), \quad (45)$$

$$p = \frac{\gamma_0 + 2 + \frac{\alpha}{2} + (\nu_j^2 D_0 E^\alpha)/(R_h^2 V_0)}{3 + \frac{\alpha}{2}}, \quad (46)$$

$$\xi^2 = \frac{z^2 (3+\frac{\alpha}{2}) V_0}{2 D_0 E^\alpha}, \quad (47)$$

$$\xi_h^2 = \frac{z_h^2 (3+\frac{\alpha}{2}) V_0}{2 D_0 E^\alpha}, \quad (48)$$

${}_1F_1(a,b,x)$ is again a confluent hypergeometrical function, and J_0 and J_1 are Bessel functions with $J_0(\nu_j) = 0$. R_h is the radius of the halo volume. For the CR source distribution, $f(R)$, we take first the distribution of supernova remants derived by Kodaira (1974), as used by Dogiel & Urysson (1988) and Stecker & Jones (1977), which is approximately given by

$$f(R) = (R/R_\odot)^a \exp[-b(R-R_\odot)/R_\odot], \quad \text{with} \quad a = 1.2 \quad \text{and} \quad b = 3.2. \quad (49)$$

This distribution is shown in Fig. 4a, together with examples of our modelling (45), and the CR distribution deduced from the COS-B data. The model includes a large halo: $R_h = 30$ kpc and $z_h = 20$ kpc. Predictions are presented for $E = 1$ and 100 GeV and $V_0 = 10$ and 0.001 km s^{-1} kpc^{-1}. Other parameter values are given in the figure. The corresponding z profiles near $R = R_\odot$ are shown in Fig. 4b. For the model with $V_0 = 0.001$ km s^{-1} kpc^{-1}, the quantity ξ_h is $\ll 1$, both at 1 and 100 GeV, so diffusion dominates. As expected (Sect. 2.2), the CR distributions for $E = 1$ and 100 GeV are identical in this case. For the models with $V_0 = 10$ km s^{-1} kpc^{-1}, convection plays a non-negligible role ($\xi_h \approx 6$ at 1 GeV). In this case, it is evident from Fig. 4a that the radial distribution of particles with $E \lesssim 10$ GeV (responsible for the bulk of the γ-ray emission in the Galactic disk), is inconsistent with the observed distribution. The discrepancy would be larger for $D_0 \approx (0.5-3) \times 10^{28}$ cm^2 s^{-1}, as derived in Sect. 5. Increasing the values of z_h and R_h would have a marginal impact.

It can be concluded that a model in which diffusion, rather than convection, plays a dominant role is preferred by the observed weak CR gradient (if the CR source distribution indeed resembles that of the SNR distribution used). The reason is that the inclusion of convection leads to a smaller effective diffusion halo compared to the halo in the pure diffusion model, as can be seen in Fig. 4b (discussed in Sect. 2.2). Hence, with increasing wind speed, the CR distribution would be more and more similar to the source distribution, as argued above. In order to reconcile the V_0 and D_0 values obtained in Sect. 5 with the weak CR gradient, the CR source distribution has to be similar to the observed distribution of CR particles. A CR source distribution with a radial exponential scale length $\gtrsim 10$ kpc (at least for $R \gtrsim 5$ kpc) is consistent with these V_0 and D_0 values.

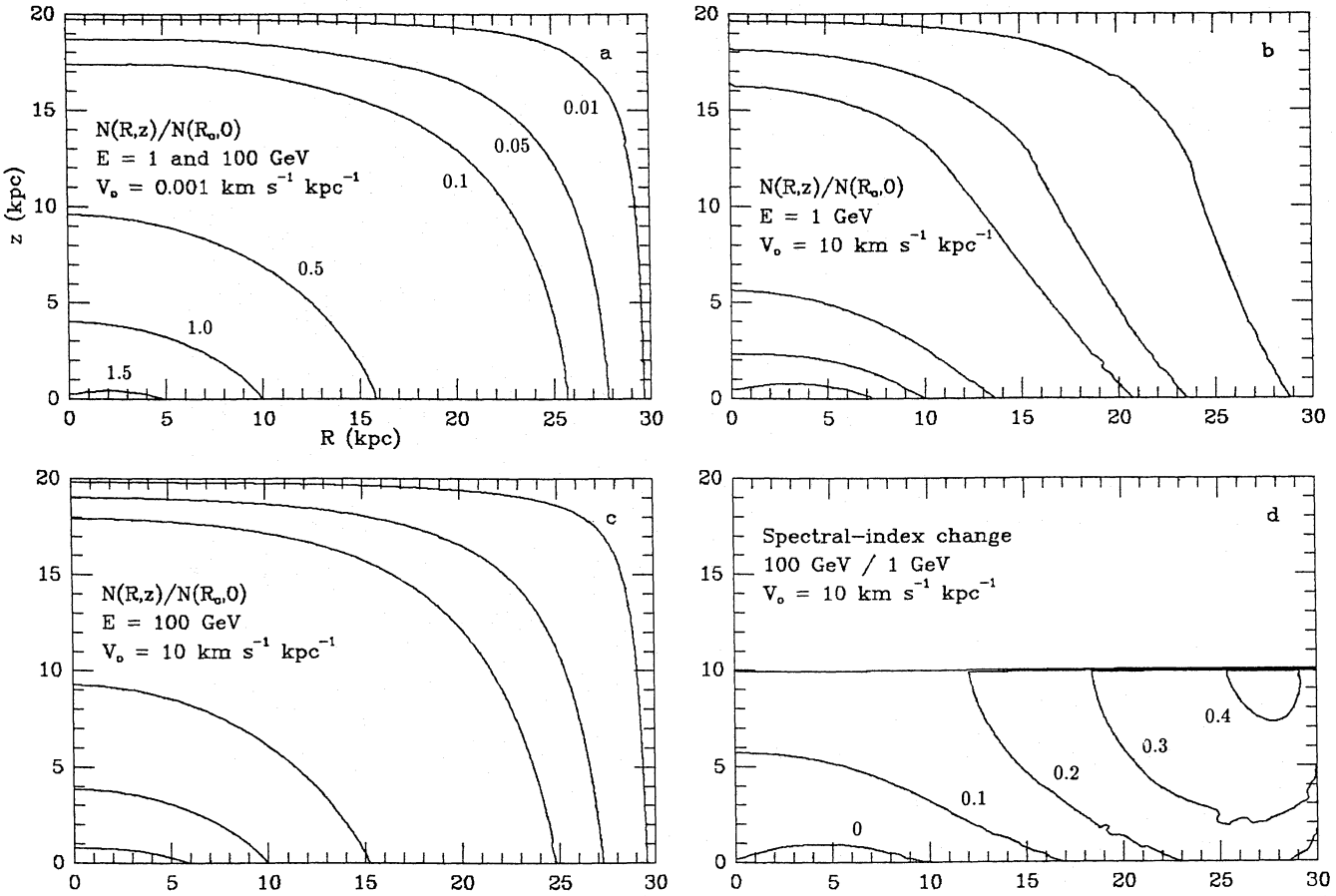

Fig. 5. a–c Two-dimensional CR density distributions for $E = 1$ and 100 GeV in convection-diffusion models with $V_0 = 10$ and 0.001 km s^{-1} kpc^{-1} (the latter approaches the pure diffusion model). A SNR-like CR source distribution was chosen, as shown in Fig. 4a. Other parameter values are the same as in Fig. 4. **d** Spectral-index changes Δs (100 GeV/1 GeV) in the model with $V_0 = 10$ km s^{-1} kpc^{-1}, relative to the spectrum at ($R = R_\odot, z = 0$). Positive Δs values imply harder spectra. Spectral distribution at $z > 10$ kpc is not shown

Because of strong selection effects, the radial distribution of SNR's in our Galaxy is, in fact, not well known. Recent studies indicate that a radial (exponential) scale length of ~ 10 kpc (assuming $R_\odot = 10$ kpc) cannot be excluded (Li et al. 1991; D. Green, priv. comm.). The same holds for pulsars. The Galactocentric distribution presented by Lyne et al. (1985) is consistent with the distribution given by Eq. (49), but a weaker fall-off with radius cannot be excluded. Both for SNR's and pulsars, however, the upper limit on the radial scale length appears to be ~ 10 kpc.

6.2. The γ-ray spectral-index distribution

The COS-B γ-ray observations in the energy range 300 MeV–6 GeV show a spectral hardening with increasing latitude in the general direction of the outer Galaxy direction, systematically over the entire second and third Galactic quadrants, which is not seen in the inner-Galaxy direction (Bloemen et al. 1988). It was pointed out by Bloemen et al. that a potential explanation is offered by the convection-diffusion model. Indeed, we saw in Sect. 2 (a confirmation of the findings by Lerche and Schlickeiser 1982) that the proton spectrum shows a flattening with increasing z (see Fig. 2 and Fig. 4b), which will be reflected in the γ-ray production spectra. Evidently, the net effect may only be substantial if the hardening of the CR spectra occurs sufficiently close to the Galactic disk, because the gas density in the Galactic halo is small. This possibility is studied here.

Figure 5 shows two-dimensional solutions of our modelling for $E = 1$ and 100 GeV and $V_0 = 0.001$ and 10 km s^{-1} kpc^{-1}, together with a spectral-index map for $V_0 = 10$ km s^{-1} kpc^{-1}. A CR source distribution as given by Eq. (49) was used. It is clear from Fig. 5d that the spectral hardening occurs at several kpc from the midplane, so the impact on γ-ray intensity spectra can be expected to be small for the local Galactic D_0 and V_0 values obtained in Sect. 5.

An accurate determination of the two-dimensional distribution of γ-ray production spectra is a considerable task. We restrict ourselves here to a simple approximation, which is sufficient to show the maximum of the spectral changes that can be expected. Because the π°-decay γ-ray emission in the energy range 300 MeV – 5 GeV is mainly produced by CR protons with energies between about 1 GeV and several tens of GeV, we can obtain reasonable insight into the γ-ray spectral behaviour as a function of latitude by comparing the γ-ray predictions from 1 GeV and 100 GeV CR protons. We have constructed for this purpose a coarse (axisymmetric) model of the gas distribution, based on scale heights and radial density profiles inferred from a variety of studies of neutral atomic gas, molecular gas, and ionized gas. We skip a detailed discussion of this gas model, because the uncertainties have no strong impact on our conclusions. The building blocks are summarized in Table 1. We then integrated the product of gas density and CR density ($E = 1$ and 100 GeV) along different lines of sight. This integral is a measure of the γ-ray

Table 1. Outline of the Galactic gas model used in Sect. 6

Component	$R \leqq R_\odot$	$R_\odot < R < 1.5\,R_\odot$	$1.5\,R_\odot < R < 25$ kpc	Notes
Cold H I and warm cloud envelopes	$h = 135$ pc	135 → 330	330 → 1500	(a)
	$n_0 = 0.37\,\mathrm{cm}^{-3}$	0.37 → 0.15	0.15 → 0	(b)
Warm H I	$h = 400$ pc	400	400 → 1500	(c)
	$n_0 = 0.1\,\mathrm{cm}^{-3}$	0.1	0.1 → 0	
Molecular gas	$h = 60$ pc	60	–	(a)
	$n_0(R)$	$n_0(R)$	0	(d)
Ionized gas	$h = 1$ kpc	1	–	(c)
	$n_0 = 0.03\,\mathrm{cm}^{-3}$	$n_0 = 0.03$	0	
Halo gas	$h = 5$ kpc	5	5	(c)
	$n_0 = 0.005\,\mathrm{cm}^{-3}$	0.005	0.005 → 0	

Notes: (a) Gaussian distribution: $n(z) = n_0 \exp[-\frac{1}{2}(z/h)^2]$. (b) For $R < 4$ kpc assumed to decrease linearly to zero at $R = 0$. (c) Exponential distribution: $n(z) = n_0 \exp[-z/h]$. (d) $n_0(R) = 3.0$, 0.3, 0.6, 0.6, 1.2, 1.8, 1.6, 1.5, 1.2, 0.8, 0.6, 0.5, 0.4, 0.3, 0.2, 0.1 at $R = 0, 1, 2, \ldots, 15$ kpc.

intensity. We find that the variations in the spectral index are weak (a few percent) and much smaller than the observed effect.

In principle, we could introduce a radial dependence of the wind speed (increasing with radius) and/or diffusion coefficient (decreasing with radius) and thus account for the hardening of the γ-ray spectrum with latitude, but then we encounter problems explaining the weak CR gradient in case of a SNR-like source distribution. A hardening of the CR spectrum sufficiently close to the Galactic disk requires, say, $z_c(1\,\mathrm{GeV}) \approx 500$ pc. From (17) it follows that in this case $V_0 \approx 80\,\mathrm{km\,s^{-1}\,kpc^{-1}}\,(D_0/10^{28}\,\mathrm{cm^2\,s^{-1}})$. In order to limit the convection speed within a few kpc from the plane to reasonable values of $\lesssim 100\,\mathrm{km\,s^{-1}}$, this requires $D_0 \lesssim 10^{27}\,\mathrm{cm^2\,s^{-1}}$.

7. Summary and conclusions

We have discussed a two-dimensional model of the propagation of CR nuclei in galaxies, in which cosmic rays, produced in the galactic plane, diffuse into a halo and are convected outward in a galactic wind. Analytical solutions of the convection-diffusion equation are presented for

(a) protons and low-energy electrons (Appendix A and Sect. 2),
(b) nuclei subject to fragmentation (Appendix B and Sect. 3), and
(c) radioactive nuclei (Appendix C and Sect. 4),

assuming a linear increase of the convection velocity with distance from the plane ($V = 3\,V_0\,z$) and allowing for an energy-dependent diffusion coefficient ($D = D_0\,(E/\mathrm{GeV})^\alpha$). As boundary conditions the CR density is adopted to be equal to zero at the halo edges ($R = R_h$ and $z = z_h$), independent of energy. Particularly the constraint for $z = z_h$ might be important in the framework of the present study, but we find that it has no significant impact on our findings, because the CR density decreases rapidly beyond some distance $z_c < z_h$ from the plane if convective transport plays an important role.

The solutions of the transport equations are found to be characterized by two dimensionless parameters

$$\xi^2 = \frac{z^2}{z_c^2(E)} \quad \text{and} \quad \xi_h^2 = \frac{z_h^2}{z_c^2(E)},$$

with

$$z_c(E) = \sqrt{\frac{2D_0 E^\alpha}{(3+\frac{\alpha}{2})V_0}}.$$

In the limit $\xi_h \ll 1$, our model approaches the pure diffusion model. Convection plays an important role if $\xi_h \gg 1$. The parameter z_c is basically the boundary between a diffusion dominated regime ($z < z_c$) and a convection dominated regime ($z > z_c$). Because of the strong decrease of the CR density beyond z_c, this is in fact the boundary of an effective diffusion halo. The increase of the size of this effective diffusion halo with energy ($z_c \propto E^{\alpha/2}$) results from the increase of the diffusion coefficient with energy. We find that, in first order approximation, the characteristics of the convection-diffusion model can be understood if the halo boundary z_h in the classical diffusion model is replaced by the (energy-dependent) boundary z_c. For instance, the CR grammage $X \propto z_h(D_0 E^\alpha)^{-1}$ if $\xi_h \ll 1$ and $X \propto z_c(D_0 E^\alpha)^{-1} \propto (V_0 D_0 E^\alpha)^{-1/2}$ if $\xi_h \gg 1$ (Sect. 3) and the fraction f of non-decayed radioactive nuclei of a certain isotope is given by $f \approx \sqrt{D_0 \tau}/z_h$ if $\xi_h \ll 1$ (for $D = D_0$) and $f \propto \sqrt{D_0 \tau}/z_c \propto \sqrt{V_0 \tau}$ if $\xi_h \gg 1$ (Sect. 4). The CR spectral characteristics in the Galactic disk are summarized in Fig. 6.

We have derived constraints on the model parameters from cosmic-ray observations and γ-ray observations of the Milky Way. A comparison of model predictions with the observed grammage traversed by cosmic rays and the abundance of radioactive ^{10}Be indicates that $V_0 \lesssim 15\,\mathrm{km\,s^{-1}\,kpc^{-1}}$ and $D_0 \approx (0.5\text{–}3) \times 10^{28}\,\mathrm{cm^2\,s^{-1}}$. Furthermore, we conclude from the CR observations that the effective CR scale height in the solar vicinity has to be less than ~ 3 kpc.

We find that the very weak Galacto-centric CR gradient, deduced from γ-ray analyses, indicates that these parameter values may not be representative for the Galaxy as a whole, unless the radial distribution of CR sources shows a weak radial fall-off as well. If the Galactic CR source distribution resembles that of supernova-remnants or pulsars, diffusion-dominated propagation in an extensive halo, rather than convection in a wind, is suggested by the observed weak CR gradient. The reason is that the inclusion of convection leads to a smaller effective diffusion halo compared to the size of the halo in the pure diffusion model.

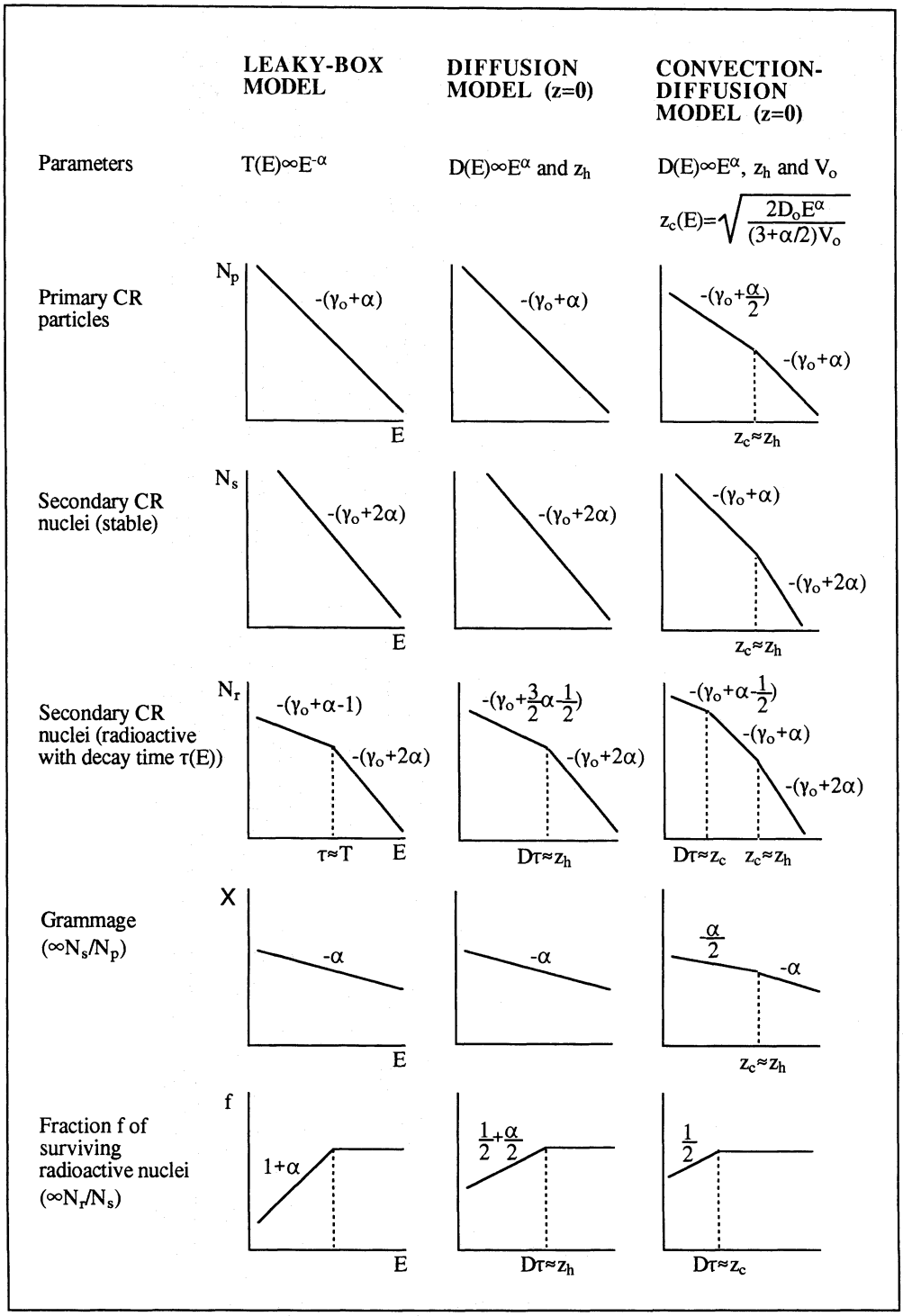

Fig. 6. Summary of asymptotic spectral indices, assuming a power-law CR source spectrum with spectral index γ_0

The expected hardening of the CR spectrum with distance from the plane (in case convective transport plays a role) may account for the observing hardening of the γ-ray spectrum with increasing latitude in the outer-Galaxy ($E_\gamma \gtrsim 300$ MeV) – assuming that the γ-ray emission is dominated by π°-decay or bremsstrahlung from low-energy electrons – if the hardening of the CR spectrum starts sufficiently close to the plane (inside the gas disk). This requires $D_0 \lesssim 10^{27}\,\mathrm{cm^2\,s^{-1}}$ in order to limit the convection speed to reasonable values of $\lesssim 100\,\mathrm{km\,s^{-1}}$ within a few kpc from the Galactic plane.

Our findings are in good agreement with the results from a recent study by Webber et al. (1992), using a convection-diffusion model with a constant wind speed.

Acknowledgements. Vladimir Dogiel acknowledges receipt of a visitors grant from the Netherlands Organization for Scientific Research (NWO) and thanks SRON Space Research Leiden for its hospitality. This work was partially supported by Grant No. 0189/89 of the NATO Scientific Affairs Division.

Appendix A: solution of the two-dimensional convection-diffusion equation for protons and low-energy electrons

We consider CR propagation in a convection-diffusion model, described by an equation of the form

$$-\nabla(\hat{D}\nabla N - \boldsymbol{V}N) - \frac{\partial}{\partial E}\left(\frac{\operatorname{div}\boldsymbol{V}}{3}EN\right) = Q(\boldsymbol{r}) \tag{A1}$$

(see Sect. 2.1), with

$$\hat{D}(E) = \begin{pmatrix} D_{RR} & D_{Rz} \\ D_{zR} & D_{zz} \end{pmatrix} = \begin{pmatrix} D_0 E^\alpha & 0 \\ 0 & D_0 E^\alpha \end{pmatrix},$$

$$V(z) = 3V_0 z,$$

$$Q(E, Rz) = 2z_s K E^{-\gamma_0}\delta(z) f(R),$$

and boundary conditions

$$N(E, R = R_h, z) = 0$$

$$N(E, R, |z| = z_h) = 0.$$

Equation (A1) can thus be written as

$$-D_0 E^\alpha\left(\frac{1}{R}\frac{\partial}{\partial R}R\frac{\partial}{\partial R}N + \frac{\partial^2}{\partial z^2}N\right) + 3V_0\frac{\partial}{\partial z}(zN) - V_0\frac{\partial}{\partial E}(EN) = Q(E, R, z). \tag{A2}$$

Writing N and $f(R)$ as series of Bessel functions

$$N(E, R, z) = \sum_{j=1}^{\infty} J_0(\nu_j R/R_h)\, C_j(E, z), \tag{A3}$$

$$f(R) = \sum_{j=1}^{\infty} J_0(\nu_j R/R_h)\frac{2\int_0^1 x J_0(\nu_j x) f(x R_h)\,dx}{J_1^2(\nu_j)}, \tag{A4}$$

with $J_0(\nu_j) = 0$, Eq. (A2) for each term j can be written as [3]

$$\frac{\nu_j^2 D_0 E^\alpha}{R_h^2} C_j - D_0 E^\alpha\frac{\partial^2}{\partial z^2}C_j + 3V_0\frac{\partial}{\partial z}(zC_j) - V_0\frac{\partial}{\partial E}(EC_j) = 4z_s K E^{-\gamma_0}\delta(z)\frac{\int_0^1 x J_0(\nu_j x) f(x R_h)\,dx}{J_1^2(\nu_j)} \equiv Q_j E^{-\gamma_0}\delta(z). \tag{A5}$$

Defining

$$P_j^2 = \frac{\nu_j^2 D_0}{R_h^2 V_0} \tag{A6}$$

and

$$\xi = z\sqrt{\frac{(3+\tfrac{\alpha}{2})V_0}{2D_0 E^\alpha}}, \tag{A7}$$

$$\left(\frac{\partial}{\partial z} = \sqrt{\frac{(3+\tfrac{\alpha}{2})V_0}{2D_0 E^\alpha}}\frac{\partial}{\partial\xi} \quad \text{and} \quad \frac{\partial}{\partial E} = \frac{\partial}{\partial E} - \frac{\alpha}{2}\frac{\xi}{E}\frac{\partial}{\partial\xi}\right)$$

[3] For Bessel functions

$$\frac{1}{R}\frac{\partial}{\partial R}R\frac{\partial}{\partial R}J_0(\nu_j R/R_h) = -\left(\frac{\nu_j}{R_h}\right)^2 J_0(\nu_j R/R_h).$$

Eq. (A5) is equivalent to

$$\frac{\partial^2}{\partial\xi^2}C_j - 2\xi\frac{\partial C_j}{\partial\xi} + \frac{2}{3+\frac{\alpha}{2}}\left(\frac{\partial}{\partial E}(EC_j) - 3C_j - P_j^2 E^\alpha C_j\right) = -\sqrt{\frac{2}{(3+\frac{\alpha}{2})D_0 V_0}}\, Q_j E^{-(\gamma_0+\alpha/2)}\delta(\xi). \tag{A8}$$

Define $C_j = K_j(E, \xi)\,\varphi_j(E)$ and choose φ_j to satisfy the condition

$$\left(E\frac{\partial\varphi_j}{\partial E} - 3\varphi_j - P_j^2 E^\alpha\varphi_j\right)K_j = 0. \tag{A9}$$

This gives

$$\varphi_j(E) = E^3\exp(P_j^2 E^\alpha/\alpha). \tag{A10}$$

Eq. (A8) can then be written as

$$\frac{\partial^2}{\partial\xi^2}K_j - 2\xi\frac{\partial K_j}{\partial\xi} + \frac{2}{3+\frac{\alpha}{2}}\frac{\partial}{\partial E}(EK_j) = -\sqrt{\frac{2}{(3+\frac{\alpha}{2})D_0 V_0}}\frac{Q_j E^{-(\gamma_0+\alpha/2)}\delta(\xi)}{\varphi_j(E)} = -\sqrt{\frac{2}{(3+\frac{\alpha}{2})D_0 V_0}}\, Q_j E^{-(\gamma_0+\alpha/2+3)}\exp\left(-\frac{P_j^2 E^\alpha}{\alpha}\right)\delta(\xi). \tag{A11}$$

Representing the exponential term as a series

$$\exp\left(-\frac{P_j^2 E^\alpha}{\alpha}\right) = \sum_{n=0}^{\infty}\frac{(-1)^n}{n!}\left(\frac{P_j^2 E^\alpha}{\alpha}\right)^n, \tag{A12}$$

K_j can be written as

$$K_j = \sum_n K_j^n. \tag{A13}$$

Then we have for each term of K_j

$$\frac{\partial^2}{\partial\xi^2}K_j^n - 2\xi\frac{\partial K_j^n}{\partial\xi} + \frac{2}{3+\frac{\alpha}{2}}\frac{\partial}{\partial E}(EK_j^n) = 0, \tag{A14}$$

with boundary conditions

$$2\frac{\partial K_j^n}{\partial\xi}\bigg|_{\xi=0} = -\sqrt{\frac{2}{(3+\frac{\alpha}{2})D_0 V_0}} \cdot Q_j E^{-(\gamma_0+\alpha/2+3-\alpha n)}\frac{(-1)^n}{n!}\left(\frac{P_j^2}{\alpha}\right)^n \tag{A15a}$$

$$K_j^n|_{\xi=\xi_h} = 0. \tag{A15b}$$

The eigenfunctions of Eq. (A14) in E are power-law functions of the kind $E^{-\lambda}$

$$K_j^n(\xi, E) = K_{j\lambda}^n(\xi)\,E^{-\lambda}.$$

For each $K_{j\lambda}^n$ we have

$$\frac{\partial^2}{\partial\xi^2}K_{j\lambda}^n - 2\xi\frac{\partial K_{j\lambda}^n}{\partial\xi} - \frac{(\lambda-1)}{2(3+\frac{\alpha}{2})}K_{j\lambda}^n = 0.$$

Independent solutions can be represented as

$$K_{j\lambda}^n = C_1 y_\lambda^1 + C_2 y_\lambda^2,$$

with

$$y_\lambda^1 = {}_1F_1\left(\frac{p}{2}, \frac{1}{2}, \xi^2\right)$$

$$y_\lambda^2 = \xi\, {}_1F_1\left(\frac{p+1}{2}, \frac{3}{2}, \xi^2\right)$$

$$p = \frac{\lambda - 1}{2\,(3+\frac{\alpha}{2})},$$

where ${}_1F_1\,(a,b,x)$ is a confluent hypergeometrical function. The constants C_1 and C_2 can be determined from the boundary conditions (A15a, b). Defining $f_1^\lambda = y_\lambda^1 E^{-\lambda}$ and $f_2^\lambda = y_\lambda^2 E^{-\lambda}$, we have at $\xi = 0$

$$\frac{\partial f_1^\lambda}{\partial \xi} = 0 \qquad \text{for any} \quad \lambda$$

$$\frac{\partial f_2^\lambda}{\partial \xi} \propto E^{-\lambda}.$$

In order to satisfy the first boundary condition (A15a) we should put the only value for $\lambda\,(\equiv\lambda^*)$ at f_2^λ

$$\lambda^* = \gamma_0 + 3 + \tfrac{\alpha}{2} - \alpha n$$

$$C_2 = -\frac{Q_j}{2}\,\frac{(-1)^n}{n!}\left(\frac{P_j^2}{\alpha}\right)^n \sqrt{\frac{2}{(3+\frac{\alpha}{2})\,D_0\,V_0}}.$$

So the general solution is

$$K_j^n = C_2^{\lambda^*}\, f_2^{\lambda^*} + \sum_\lambda C_1^\lambda\, f_1^\lambda.$$

We can represent the second boundary condition (A15b) as

$$K_j^n\,(z = z_h, E) = -\frac{Q_j}{2D_0}\,\frac{(-1)^n}{n!}\left(\frac{P_j^2}{\alpha}\right)^n z_h\, E^{-\lambda^* - \alpha/2}$$
$$\cdot\left({}_1F_1\left(\frac{p^*+1}{2}, \frac{3}{2}, z_h^2\,\frac{(3+\frac{\alpha}{2})\,V_0}{2D_0\,E^\alpha}\right) - \sum_{\nu=0}^{\infty} C_\nu\, E^{-\lambda_\nu + \lambda^* + \alpha/2}\, {}_1F_1\right.$$
$$\left.\cdot\left(\frac{p_\nu}{2}, \frac{1}{2}, z_h^2\,\frac{(3+\frac{\alpha}{2})\,V_0}{2D_0\,E^\alpha}\right)\right) = 0.$$

This boundary condition requires that $E^{-\lambda_\nu + \lambda^* + \alpha/2}$ is an integer power of $E^{-\alpha}$, namely $\lambda_\nu = \lambda^* + \frac{\alpha}{2} + \alpha\nu\,(\nu = 0, 1, 2, \ldots)$. Then

$$K_j^n = \frac{Q_j}{2D_0}\,\frac{(-1)^n}{n!}\left(\frac{P_j^2}{\alpha}\right)^n z_h\, E^{-\lambda^* - \alpha/2} \tag{A17}$$
$$\cdot\left(-{}_1F_1\left(\frac{p^*+1}{2}, \frac{3}{2}, \xi^2\right)\frac{z}{z_h} + \sum_{\nu=0}^{\infty} C_\nu\, E^{-\alpha\nu}\, {}_1F_1\left(\frac{p_\nu}{2}, \frac{1}{2}, \xi^2\right)\right).$$

Using a series representation of ${}_1F_1$

$${}_1F_1\,(a,b,x) = \sum_{n=0}^{\infty} \frac{x^n\,(a)_n}{n!\,(b)_n}, \qquad (A)_n \equiv (A+n-1)\cdot\ldots(A+1)\,A,$$

the coefficients C_ν follow one by one from the condition

$${}_1F_1\left(\frac{p^*+1}{2}, \frac{3}{2}, \frac{a z_h^2}{E^\alpha}\right) = \sum_{\nu=0}^{\infty} C_\nu\, E^{-\alpha\nu}\, {}_1F_1\left(\frac{p_\nu}{2}, \frac{1}{2}, \frac{a z_h^2}{E^\alpha}\right)$$

$$\left(\text{where } a = \frac{(3+\frac{\alpha}{2})\,V_0}{2D_0}\right),$$

namely $C_0 = 1$ and for $\nu > 0$

$$C_\nu = \frac{(-1)^\nu\,((p^*+1)/2)_\nu\,(a z_h^2)^\nu}{\nu!\,(\frac{3}{2})_\nu}$$
$$-\sum_{l=1}^{\nu-1}\frac{(-1)^{\nu-l}\,C_l\,(p_\nu/2)_{\nu-l}\,(a z_h^2)^{\nu-l}}{(\nu-l)!\,(\frac{1}{2})_{\nu-l}}.$$

Equation (A17) provides the exact solution $N(E, R, z)$ for isotropic diffusion with boundary conditions at $z = z_h$ and $R = R_h$. For $\gamma_0 \gg \alpha$, however, the full solution of (A2) can be approximated by

$$N(E,R,z) = \frac{2 z_s K E^{-(\gamma_0+\alpha)}}{D_0}\sum_{j=1}^{\infty} J_0\,(\nu_j R/R_h)$$
$$\cdot\frac{\int_0^1 x J_0\,(\nu_j x)\, f(x R_h)\,dx}{J_1^2\,(\nu_j)}\,\exp\left(\frac{P_j^2 E^\alpha}{\alpha}\right)$$
$$\cdot\sum_{n=0}^{\infty}\frac{(-1)^n}{n!}\left(\frac{P_j^2 E^\alpha}{\alpha}\right)^n$$
$$\cdot\left(z_h\,\frac{{}_1F_1\,((p_n+1)/2, \frac{3}{2}, \xi_h^2)}{{}_1F_1\,(p_n/2, \frac{1}{2}, \xi_h^2)}\,{}_1F_1\left(\frac{p_n}{2}, \frac{1}{2}, \xi^2\right)\right.$$
$$\left.-\,z\,{}_1F_1\left(\frac{p_n+1}{2}, \frac{3}{2}, \xi^2\right)\right), \tag{A18}$$

with

$$p_n = \frac{\gamma_0 + 2 + \frac{\alpha}{2} - \alpha n}{3+\frac{\alpha}{2}}.$$

An approximation

The exact solution of Eq. (A1) is much simpler for anisotropic diffusion, with a diffusion coefficient of the form

$$\hat{D} = \begin{pmatrix} D_{RR} & D_{Rz} \\ D_{zR} & D_{zz} \end{pmatrix} = \begin{pmatrix} D_0 & 0 \\ 0 & D_0\,E^\alpha \end{pmatrix}.$$

It can be represented in the same form as (A11), with the only difference that $\varphi_j(E)$ is now given by

$$\varphi_j(E) = E^{3+P_j^2} \tag{A19}$$

instead of (A10), with P_j^2 defined by (A6). The equivalent of (A18) is then

$$N(E,R,z) = \frac{2 z_s K E^{-(\gamma_0+\alpha)}}{D_0}$$
$$\cdot\sum_{j=1}^{\infty} J_0\,(\nu_j R/R_h)\,\frac{\int_0^1 x J_0\,(\nu_j x)\, f(x R_h)\,dx}{J_1^2\,(\nu_j)} \tag{A20}$$
$$\cdot\left(z_h\,\frac{{}_1F_1\,((p+1)/2, \frac{3}{2}, \xi_h^2)}{{}_1F_1\,(p/2, \frac{1}{2}, \xi_h^2)}\,{}_1F_1\left(\frac{p}{2}, \frac{1}{2}, \xi^2\right) - z\,{}_1F_1\left(\frac{p+1}{2}, \frac{3}{2}, \xi^2\right)\right),$$

where

$$p = \frac{\gamma_0 + 2 + \frac{\alpha}{2} + \nu_j^2\,D_0/(R_h^2\,V_0)}{3+\frac{\alpha}{2}},$$

$$\xi^2 = \frac{z^2\,(3+\frac{\alpha}{2})\,V_0}{2D_0\,E^\alpha},$$

$$\xi_h^2 = \frac{z_h^2\,(3+\frac{\alpha}{2})\,V_0}{2D_0\,E^\alpha}.$$

This solution for anisotropic diffusion can be used as an approximation for isotropic diffusion by replacing p by

$$p = \frac{\gamma_0 + 2 + \frac{\alpha}{2} + \nu_j^2\,D_0\,E^\alpha/(R_h^2\,V_0)}{3+\frac{\alpha}{2}} \tag{A21}$$

(if α is sufficiently small). In the one-dimensional case (discussed in Sect. 2.2), Eq. (A20) reduces to

$$N(E,z)=\frac{z_s K E^{-(\gamma_0+\alpha)}}{D_0}\cdot\left(z_h\frac{{}_1F_1((p+1)/2,\frac{3}{2},\xi_h^2)}{{}_1F_1(p/2,\frac{1}{2},\xi_h^2)}\,{}_1F_1\left(\frac{p}{2},\frac{1}{2},\xi^2\right)-z\,{}_1F_1\left(\frac{p+1}{2},\frac{3}{2},\xi^2\right)\right),\tag{A22}$$

with

$$p=\frac{\gamma_0+2+\frac{\alpha}{2}}{3+\frac{\alpha}{2}}.\tag{A23}$$

In order to illustrate that this is a valid approximation, we compare it with the exact solution for the one-dimensional boundaryless case ($N\to 0$ for $z\to\pm\infty$), similar to the result obtained by Lerche and Schlickeiser (1982):

$$N(E,z)=\frac{E^{-(\gamma_0+\alpha/2)}}{2\sqrt{\pi V_0 D_0(\alpha+6)}}\cdot\int_0^\infty\frac{(1+\xi)}{\sqrt{\xi}}\exp\left(\frac{-V_0(6+\alpha)z^2}{4D_0E^\alpha\xi}\right)\mathrm{d}\xi,\tag{A24}$$

which has the following asymptotic behaviour

(a) if $\xi_c=\frac{V_0(6+\alpha)z^2}{4D_0E^\alpha}\ll 1$ then

$$N(E,z)\propto E^{-(\gamma_0+\alpha/2)}\left(1-z\sqrt{\frac{V_0(6+\alpha)}{4D_0E^\alpha}}\right)$$

(b) if $\xi_c\gg 1$ then

$$N(E,z)\propto E^{-(6\gamma_0+\alpha)/(6+\alpha)}\,z^{-(2\gamma_0+\alpha+4)/(6+\alpha)}.$$

These asymptotic expressions are identical to those of Eq. (A22), which are given in Sect. 2.2 (18b, c).

Appendix B: solution of the one-dimensional convection-diffusion equation for nuclei subject to fragmentation

We consider here the propagation of nuclei subject to fragmentation (discussed in Sect. 3), described by

$$-\frac{\partial}{\partial z}\left(D(E)\frac{\partial}{\partial z}N-VN\right)-\frac{\partial}{\partial E}\left(\frac{1}{3}\frac{\mathrm{d}V}{\mathrm{d}z}EN\right)+2z_g n_g v\sigma\,\delta(z)N=Q(E,z),\tag{B1}$$

using

$$D(E)=D_0E^\alpha,$$

$$V(z)=3V_0z,$$

$$Q(E,z)=2z_sKE^{-\gamma_0}\delta(z),$$

In the fragmentation term, z_g and n_g are the half thickness and average density of the gas disk, σ is the cross section of the fragmentation process, and v is the particle velocity. The boundary condition is

$$N(E,|z|=z_h)=0.$$

The solution of (B1) can be represented as a series

$$N=\sum_{n=0}^{\infty}(-1)^n\left(\frac{z_g z_h n_g v\sigma}{D_0E^\alpha}\right)^n A_n\equiv\sum_{n=0}^{\infty}N_n.\tag{B2}$$

For $N_0(E,z)$ Eq. (B1) reads

$$-\frac{\partial}{\partial z}\left(D(E)\frac{\partial}{\partial z}N_0-VN_0\right)-\frac{\partial}{\partial E}\left(\frac{1}{3}\frac{\mathrm{d}V}{\mathrm{d}z}EN_0\right)=Q(E,z),\tag{B3}$$

and

$$N_0(E,z)=\frac{z_sKE^{-(\gamma_0+\alpha)}}{D_0}\cdot\left(z_h\frac{{}_1F_1((p_0+1)/2,\frac{3}{2},\xi_h^2)}{{}_1F_1(p_0/2,\frac{1}{2},\xi_h^2)}\,{}_1F_1\left(\frac{p_0}{2}\frac{1}{2},\xi^2\right)-z\,{}_1F_1\left(\frac{p_0+1}{2},\frac{3}{2},\xi^2\right)\right)\tag{B4}$$

(as for particles not subject to fragmentation; see Sect. 2.2), with

$$p_0=\frac{\gamma_0+2+\frac{\alpha}{2}}{3+\frac{\alpha}{2}},$$

$$\xi^2=\frac{z^2(3+\frac{\alpha}{2})V_0}{2D_0E^\alpha},$$

$$\xi_h^2=\frac{z_h^2(3+\frac{\alpha}{2})V_0}{2D_0E^\alpha}.$$

For $N_n(E,z)$ Eq. (B1) reads

$$-\frac{\partial}{\partial z}\left(D(E)\frac{\partial}{\partial z}N_n-VN_n\right)-\frac{\partial}{\partial E}\left(\frac{1}{3}\frac{\mathrm{d}V}{\mathrm{d}z}EN_n\right)=2z_g n_g\sigma v\,\delta(z)N_{n-1},\tag{B5}$$

and

$$N_n(E,z)=\frac{z_sKE^{-(\gamma_0+\alpha)}}{D_0}(-1)^n\left(\frac{z_g z_h n_g v\sigma}{D_0E^\alpha}\right)^n\cdot\left(z_h\frac{{}_1F_1((p+1)/2,\frac{3}{2},\xi_h^2)}{{}_1F_1(p_n/2,\frac{1}{2},\xi_h^2)}\,{}_1F_1\left(\frac{p_n}{2},\frac{1}{2},\xi^2\right)-z\,{}_1F_1\left(\frac{p_n+1}{2},\frac{3}{2},\xi^2\right)\right)\cdot\prod_{k=0}^{n-1}\frac{{}_1F_1((p_k+1)/2,\frac{3}{2},\xi_h^2)}{{}_1F_1(p^k/2,\frac{1}{2},\xi_h^2)},\tag{B6}$$

with

$$p_k=\frac{\gamma_0+2+\alpha(k+1)/2}{3+\frac{\alpha}{2}}.\tag{B7}$$

From (B5) and (B7) we find that the sum (B2) equals

$$N(E,z)=\frac{z_sKE^{-(\gamma_0+\alpha)}}{D_0}\sum_{n=0}^{\infty}(-1)^n\left(\frac{z_g z_h n_g v\sigma}{D_0E^\alpha}\right)^n\cdot\left(z_h\frac{{}_1F_1((p_n+1)/2,\frac{3}{2},\xi_h^2)}{{}_1F_1(p_n/2,\frac{1}{2},\xi_h^2)}\,{}_1F_1\left(\frac{p_n}{2},\frac{1}{2},\xi^2\right)-z\,{}_1F_1\left(\frac{p_n+1}{2},\frac{3}{2},\xi^2\right)\right)\cdot\prod_{k=0}^{n-1}\frac{{}_1F_1((p_k+1)/2,\frac{3}{2},\xi_h^2)}{{}_1F_1(p_k/2,\frac{1}{2},\xi_h^2)},\tag{B8}$$

with the product term equal to 1 for $n=0$.

Appendix C: solution of the two-dimensional convection-diffusion equation for (radioactive) secondary nuclei

We consider here the propagation of radioactive nuclei (discussed in Sect. 4), described by

$$-V(\hat{D}\nabla N - VN) - \frac{\partial}{\partial E}\left(\frac{\mathrm{div}\, V}{3} EN\right) + \frac{N}{\tau_0 E} = Q(r), \tag{C1}$$

with

$$\hat{D}(E) = \begin{pmatrix} D_{RR} & D_{Rz} \\ D_{zR} & D_{zz} \end{pmatrix} = \begin{pmatrix} D_0 E^\alpha & 0 \\ 0 & D_0 E^\alpha \end{pmatrix},$$

$$V(z) = 3 V_0 z.$$

Equation (C1) can thus be written as

$$-D_0 E^\alpha \left(\frac{1}{R}\frac{\partial}{\partial R} R \frac{\partial}{\partial R} N + \frac{\partial^2}{\partial z^2} N\right) + 3V_0 \frac{\partial}{\partial z}(zN) - V_0 \frac{\partial}{\partial E}(EN) + \frac{N}{\tau_0 E} = Q(E, R, z). \tag{C2}$$

The decay time depends on the energy of the nuclei, $\tau(E) = \tau_r E/mc^2 \equiv \tau_0 E$, where τ_r is the life time at rest. For the production rate Q we write (see Sect. 4)

$$Q(E, R, z) = 2 z_g n_g v \sigma N_p(E, R, z)\, \delta(z),$$

where z_g and n_g are the half thickness and average density of the gas disk, σ is the effective cross section of the fragmentation process, and v is the particle velocity. $N_p(E, R, z)$ is the number density of protons determined in Appendix A (A20). As boundary conditions we set

$$N(E, R = R_h, z) = 0$$
$$N(E, R, |z| = z_h) = 0.$$

Following the same approach as in Appendix A (to which the reader is referred for various details), we write N as a series of Bessel functions

$$N(E, R, z) = \sum_{j=1}^{\infty} J_0(\nu_j R/R_h)\, C_j(E, z), \tag{C3}$$

with $J_0(\nu_j) = 0$, so that Eq. (C2) for each term of this series can be written as

$$\frac{\nu_j^2 D_0 E^\alpha}{R_h^2} C_j - D_0 E^\alpha \frac{\partial^2}{\partial z^2} C_j + 3V_0 \frac{\partial}{\partial z}(zC_j) - V_0 \frac{\partial}{\partial E}(EC_j) + \frac{C_j}{\tau_0 E} = K' E^{-(\gamma_0+\alpha)} \frac{\int_0^1 x J_0(\nu_j x)\, f(x R_h)\, dx}{J_1^2(\nu_j)} \cdot \frac{{}_1F_1((p+1)/2, \frac{3}{2}, \xi_h^2)}{{}_1F_1(p/2, \frac{1}{2}, \xi_h^2)} \delta(z) \equiv Q_j E^{-\gamma} \delta(z), \tag{C4}$$

with $K' = 4 z_g z_s z_h n_g v \sigma K$ and $\gamma = \gamma_0 + \alpha$. The parameter ξ_h^2 is defined after (A20) and p is given by (A21). Introducing, again, the parameters P_j^2 (A6) and ξ (A7), it follows for Eq. (C4)

$$\frac{\partial^2}{\partial \xi^2} C_j - 2\xi \frac{\partial C_j}{\partial \xi} + \frac{2}{3+\frac{\alpha}{2}} \cdot \left(\frac{\partial}{\partial E}(EC_j) - 3C_j - P_j^2 E^\alpha C_j - \frac{C_j}{V_0 \tau_0 E}\right) = -\sqrt{\frac{2}{(3+\frac{\alpha}{2}) D_0 V_0}}\, Q_j E^{-(\gamma+\alpha/2)} \delta(\xi). \tag{C5}$$

Define $C_j = K_j(E, \xi)\, \varphi_j(E)$ and choose φ_j to satisfy the condition

$$\left(E\frac{\partial \varphi_j}{\partial E} - 3\varphi_j - P_j^2 E^\alpha \varphi_j - \frac{\varphi_j}{V_0 \tau_0 E}\right) K_j = 0. \tag{C6}$$

This gives

$$\varphi_j(E) = E^3 \exp\left(\frac{P_j^2 E^\alpha}{\alpha} - \frac{1}{V_0 \tau_0 E}\right). \tag{C7}$$

Equation (C5) can then be written as

$$\frac{\partial^2}{\partial \xi^2} K_j - 2\xi \frac{\partial K_j}{\partial \xi} + \frac{2}{3+\frac{\alpha}{2}} \frac{\partial}{\partial E}(EK_j) = -\sqrt{\frac{2}{(3+\frac{\alpha}{2}) D_0 V_0}}\, \frac{Q_j E^{-(\gamma+\alpha/2)} \delta(\xi)}{\varphi_j(E)} = -\sqrt{\frac{2}{(3+\frac{\alpha}{2}) D_0 V_0}}\, Q_j E^{-(\gamma+\alpha/2+3)} \cdot \exp\left(\frac{1}{V_0 \tau_0 E} - \frac{P_j^2 E^\alpha}{\alpha}\right) \delta(\xi). \tag{C8}$$

Representing the exponential term as a series

$$\exp\left(\frac{1}{V_0 \tau_0 E} - \frac{P_j^2 E^\alpha}{\alpha}\right) = \sum_{n=0}^{\infty} \frac{1}{n!}\left[\left(\frac{1}{V_0 \tau_0 E}\right)^n + (-1)^n \left(\frac{P_j^2 E^\alpha}{\alpha}\right)^n\right], \tag{C9}$$

K_j can be written as

$$K_j = \sum_n (K_{1j}^n + K_{2j}^n). \tag{C10}$$

Then we have for each term of K_j

$$\frac{\partial^2}{\partial \xi^2} K_{1,2j}^n - 2\xi \frac{\partial K_{1,2j}^n}{\partial \xi} + \frac{2}{3+\frac{\alpha}{2}} \frac{\partial}{\partial E}(EK_{1,2j}^n) = 0, \tag{C11}$$

with boundary conditions

$$2\frac{\partial K_{1j}^n}{\partial \xi}\bigg|_{\xi=0} = -\sqrt{\frac{2}{(3+\frac{3}{2}) D_0 V_0}}\, Q_j E^{-(\gamma+\alpha/2+3+n)} \frac{1}{n!}\left(\frac{1}{V_0 \tau_0}\right)^n \tag{C12a}$$

$$2\frac{\partial K_{2j}^n}{\partial \xi}\bigg|_{\xi=0} = -\sqrt{\frac{2}{(3+\frac{\alpha}{2}) D_0 V_0}}\, Q_j E^{-(\gamma+\alpha/2+3-\alpha n)} \frac{(-1)^n}{n!}\left(\frac{P_j^2}{\alpha}\right)^n \tag{C12b}$$

$$K_{1,2j}^n|_{\xi=\xi_h} = 0. \tag{C12c}$$

The solutions for K_{1j}^n and K_{2j}^n are

$$K_{1j}^n = \frac{Q_j}{2D_0} E^{-(\gamma+\alpha+3+n)} \frac{1}{n!}\left(\frac{1}{V_0 \tau_0}\right)^n \cdot \left(z_h \frac{{}_1F_1((p_{1n}+1)/2, \frac{3}{2}, \xi_h^2)}{{}_1F_1(p_{1n}/2, \frac{1}{2}, \xi_h^2)} {}_1F_1\left(\frac{p_{1n}}{2}, \frac{1}{2}, \xi^2\right) - z\, {}_1F_1\left(\frac{p_{1n}+1}{2}, \frac{3}{2}, \xi^2\right)\right), \tag{C13}$$

$$K_{2j}^{n} = \frac{Q_j}{2D_0} E^{-(\gamma+\alpha+3-\alpha n)} \frac{(-1)^n}{n!} \left(\frac{P_j^2}{\alpha}\right)^n \tag{C14}$$

$$\cdot \left(z_h \frac{{}_1F_1((p_{2n}+1)/2, \frac{3}{2}, \xi_h^2)}{{}_1F_1(p_{2n}/2, \frac{1}{2}, \xi_h^2)} {}_1F_1\left(\frac{p_{2n}}{2}, \frac{1}{2}, \xi^2\right) \right.$$

$$\left. - z \, {}_1F_1\left(\frac{p_{2n}+1}{2}, \frac{3}{2}, \xi^2\right) \right),$$

where

$$p_{1n} = \frac{\gamma+2+\frac{\alpha}{2}+n}{3+\frac{\alpha}{2}} \quad \text{and} \quad p_{2n} = \frac{\gamma+2+\frac{\alpha}{2}-\alpha n}{3+\frac{\alpha}{2}}. \tag{C15}$$

${}_1F_1(a,b,x)$ is a confluent hypergeometrical function. The full solution of Eq. (C2) can then be written as

$$N(E,R,z) = \frac{K' E^{-(\gamma+\alpha)}}{2D_0} \sum_{j=1}^{\infty} J_0(\nu_j R/R_h) \frac{\int_0^1 x J_0(\nu_j x) f(x R_h) \mathrm{d}x}{J_1^2(\nu_j)}$$

$$\cdot \frac{{}_1F_1((p+1)/2, \frac{3}{2}, \xi_h^2)}{{}_1F_1(p/2, \frac{1}{2}, \xi_h^2)} \exp\left(\frac{P_j^2 E^\alpha}{\alpha} - \frac{1}{V_0 \tau_0 E}\right)$$

$$\cdot \sum_{n=0}^{\infty} \frac{1}{n!} \left[\left(\frac{1}{V_0 \tau_0 E}\right)^n \left(z_h \frac{{}_1F_1((p_{1n}+1)/2, \frac{3}{2}, \xi_h^2)}{{}_1F_1(p_{1n}/2, \frac{1}{2}, \xi_h^2)} \right.\right.$$

$$\left. \cdot {}_1F_1\left(\frac{p_{1n}}{2}, \frac{1}{2}, \xi^2\right) - z \, {}_1F_1\left(\frac{p_{1n}+1}{2}, \frac{3}{2}, \xi^2\right) \right)$$

$$+ (-1)^n \left(\frac{P_j^2 E^\alpha}{\alpha}\right)^n \left(z_h \frac{{}_1F_1((p_{2n}+1)/2, \frac{3}{2}, \xi_h^2)}{{}_1F_1(p_{2n}/2, \frac{1}{2}, \xi_h^2)} \right.$$

$$\left.\left. \cdot {}_1F_1\left(\frac{p_{2n}}{2}, \frac{1}{2}, \xi^2\right) - z \, {}_1F_1\left(\frac{p_{2n}+1}{2}, \frac{3}{2}, \xi^2\right) \right) \right]. \tag{C16}$$

The second term in the series can be neglected if the vertical extent z_h of the halo is much smaller than the radial extent R_h, because in this case $R_h^2/(D_0 E^\alpha) \gg \tau_0 E$. It follows that for a certain point in the plane $(R, z=0)$

$$N(E) = \frac{z_h K' E^{-(\gamma+\alpha)}}{2D_0} \sum_{j=1}^{\infty} J_0(\nu_j R/R_h)$$

$$\cdot \frac{\int_0^1 x J_0(\nu_j x) f(x R_h) \mathrm{d}x}{J_1^2(\nu_j)} \frac{{}_1F_1((p+1)/2, \frac{3}{2}, \xi_h^2)}{{}_1F_1(p/2, \frac{1}{2}, \xi_h^2)} \tag{C17}$$

$$\cdot \exp\left(-\frac{1}{V_0 \tau_0 E}\right) \sum_{n=0}^{\infty} \frac{1}{n!} \left(\frac{1}{V_0 \tau_0 E}\right)^n \frac{{}_1F_1((p_{1n}+1)/2, \frac{3}{2}, \xi_h^2)}{{}_1F_1(p_{1n}/2, \frac{1}{2}, \xi_h^2)},$$

which has the following asymptotic behaviour

(a) $N(E) \propto E^{-(\gamma+\alpha)} \propto E^{-(\gamma_0+2\alpha)}$ for $z_h^2/D(E) < 1/V_0 < \tau(E)$

(b) $N(E) \propto E^{-(\gamma+\alpha/2)} \propto E^{-(\gamma_0+\alpha)}$ for $1/V_0 < z_h^2/D(E), \tau(E)$

(c) $N(E) \propto E^{-(\gamma+\alpha/2-1/2)} \propto E^{-(\gamma_0+\alpha-1/2)}$ for $\tau(E) < 1/V_0 < z_h^2/D(E)$.

References

Abramowitz M., Stegun I.A., 1972, Handbook of Mathematical Functions. Dover Publications, New York

Axford W.I., 1981, in: Origin of Cosmic Rays, Setti G., Spada G., Wolfendale A.W. (eds.). Reidel, Dordrecht, p. 339

Berezinsky V.S., Bulanov S.V., Ginzburg V.L., Dogiel V.A., Ptuskin V.S., 1990, in: Astrophysics of Cosmic Rays, Ginzburg V.L. (ed.). North Holland

Bregman J.N., 1980, ApJ 236, 577

Breidtschwerdt D., McKenzie J.F., Völk H.J., 1987, in: Interstellar Magnetic Fields, Beck R., Gräve R. (eds.). Springer, Heidelberg, p. 131

Bloemen J.B.G.M., 1989, ARA&A 27, 469

Bloemen J.B.G.M., 1991a, in: The interpretation of modern synthesis observations of spiral galaxies, Duric N., Crane P.C. (eds.). ASP, San Francisco, p. 27

Bloemen J.B.G.M., Dogiel V.A., Dorman V.L., Ptuskin V.S., 1991b, Izv. AN USSR (ser. fizich) 55, 2052

Bloemen J.B.G.M., Reich P., Reich W., Schlickeiser R., 1988, A&A 204, 88

Bloemen J.B.G.M., Strong A.W., Blitz L., Cohen R.S., Dame T.M., Grabelsky T.M., Hermsen W., Lebrun F., Mayer-Hasselwander H.A., Thaddeus P., 1986, A&A 154, 25

Bulanov S.V., Dogiel V.A., Syrovatskii S.I., 1972, osmich. Issled. 10, 532 (English trans: 1972, Comis Res. 10, 478)

Cesarsky C.J., 1980, ARA&A 18, 289

Cesarsky C.J., 1987, Proc. 20th Int. Cosmic Ray Conf. 8, 87

Chevalier R.A., Oegerle W.R., 1979, ApJ 227, 398

Clifton T.R., Frail D.A., Kulkarni S.R., Weisberg J.M., 1988, ApJ 333, 332

Dame T.M., Ungerechts H., Cohen R.S., de Geus E., Grenier I., May J., Murphy D.C., Nyman L.-A., Thaddeus P., 1987, ApJ 322, 706

Dogiel V.A., Gurevich A.V., Zybin K.P., 1992, A&A (in press)

Dogiel V.A., Kovalenko V.M., Prishchep V.L., 1980, Pis'ma A Zh (SvA Lett.) 6, 696

Dogiel V.A., Uryson A.V., 1988, A&A 197, 335

Freedman I., Giler M., Kearsey S., Osborne J.L., 1980, A&A 82, 110

Ginzburg V.L., Syrovatskii S.I., 1964, The Origin of Cosmic Rays, Pergamon Press, Oxford

Heiles C., 1989, ApJ 336, 808

Hillas A.M., 1975, Phys. Rep. 2, 59

Hummel E., Dettmar R.-J., 1990, A&A 236, 33

Hummel E., Dahlem M., van der Hulst J.M., Sukumar S., 1991, A&A 246, 10

Ipavich F., 1975, ApJ 196, 107

Jokipii J.R., 1976, ApJ 208, 900

Jones F.C., 1979, ApJ 229, 747

Kerr F.J., Bowers P.F., Jackson P.D., Kerr M., 1986, A&AS 66, 373

Kóta J., Owens A.J., 1980, ApJ 237, 814

Lerche I., Schlickeiser R., 1982, MNRAS 201, 1041

Li Z., Wheeler J.C., Bash F.N., Jeffreys W.H., 1991, ApJ 378, 93

Lyne A.G., Manchester R.N., Taylor J.H., 1985, MNRAS 213, 613

Mathews W.G., Baker J.C., 1971, ApJ 170, 241

McKee C.F., Ostriker J.P., 1977, ApJ 218, 148

Owens A.J., Jokipii J.R., 1977, ApJ 215, 677

Prishchep V.L., Ptuskin V.S., 1975, Ap&SS 32, 265

Prishchep V.L., Ptuskin V.S., 1979, Proc. 16th Int. Cosmic Ray Conf. 2, 137

Ptuskin V.S., Soutoul A., 1990, A&A 237, 445
Reich P., Reich W., 1988, A&A 196, 211
Shapiro P.R., Field G.B., 1976, ApJ 205, 762
Simpson J.A., Garcia-Munoz M., 1988, Space Sci. Rev. 46, 205
Stecker F.W., Jones F., 1977, ApJ 217, 843
Strong A.W., Bloemen J.B.G.M., Dame T.M., Grenier I.A., Hermsen W., Lebrun F., Nyman L.-A., Pollock A., Thaddeus P.A., 1988, A&A 207, 1
Sukumar S., Velusamy T., 1985, MNRAS 212, 367
Webber W.R., Lee M.A., Gupta M., 1992, ApJ 390, 96
Webber W.R., Soutoul A., Ferrando P., Gupta M., 1990, ApJ 348, 611
Wentzel D.G., 1974, ARA&A 12, 71
Werner W., 1988, A&A 201, 1